Bulletin of Volcanology (2026) 88:71
https://doi.org/10.1007/s00445-026-01995-5

RESEARCH

Decade-scale recovery of the Eyjafjallajökull ice cap, Iceland, after the 2010 summit eruption

Linda Sobolewski[1] · Magnús Tumi Gudmundsson[1] · Eyjólfur Magnússon[1] · Joaquín M. C. Belart[2] · Thomas R. Walter[3] · Benjamin R. Edwards[4] · Karuna Mira Sah[5] · William Kochtitzky[6]

Received: 4 March 2026 / Accepted: 23 May 2026

Abstract

Several eruptions at glaciated volcanoes have been witnessed during the last two centuries. However, most studies have focused on understanding the volcanic products or the hazard implications. Less attention has been put into analyzing the long-term effects on the glaciers. The 2010 summit eruption of Eyjafjallajökull (Iceland) provides an excellent opportunity to study such impacts by investigating how individual areas of the ice cap have changed with time. These include (i) the summit caldera (formation of vents/lava), (ii) the southern flank (short-lived eruption fissure), and (iii) the outlet glacier Gígjökull (lava propagation). We used high-resolution satellite data acquired by Pléiades and SPOT5, complemented by airborne LiDAR, to calculate elevation and volume changes of the glacier over varying time periods between 2008 and 2024. From August 2010 to August 2014, the main vent showed an elevation increase of ~ 80 m; visible eruption impacts on the southern flank have completely vanished; Gígjökull significantly recovered. However, the ice cap overall is shrinking. The area decreased from 72.3 km^2 (2010) to 63.5 km^2 (2024), with an average elevation change of −8.3 m. The caldera and Gígjökull did not follow this trend and showed an average elevation increase of ca. 13.4 m (1.0 m/year). We hypothesize that the depressions formed by the eruption acted as traps for drifting snow in winter, resulting in a local thickening rate far exceeding the average winter accumulation. Although the recovery is exceptional, the volume still only corresponds to around 50% of the ice loss caused by the eruption.

Keywords Eyjafjallajökull · Gígjökull · Volcano-ice interactions · Remote sensing

Introduction

Although many volcanoes on Earth are covered by glaciers or somehow interact with the cryosphere, the dynamic interaction of eruptions, glacier melting, and regrowth is barely studied. One of a few exceptions is Mount St. Helens, where the formation and growth of a new glacier after the cataclysmic eruption in May 1980 were studied in detail by Schilling et al. (2004) and Walder et al. (2008). Due to its geographic location in the North Atlantic and the variety of volcanoes with frequent activity, Iceland is an excellent place to expand research on this topic. About 10% of Iceland is covered by glaciers with currently six major ice caps, including Vatnajökull, one of the largest ice caps in Europe (7720 km^2 in 2019), followed by Langjökull, Hofsjökull, Mýrdalsjökull, Drangajökull, and Eyjafjallajökull. The area of Eyjafjallajökull (66 km^2 in 2019), however, corresponds to far less than 1% of Vatnajökull (Hannesdóttir et al. 2020) (Fig. 1A). Most glaciers in Iceland are currently retreating.

Editorial responsibility: J. Smellie

✉ Linda Sobolewski
lindas@hi.is

[1] Institute of Earth Sciences, University of Iceland, Reykjavík, Iceland

[2] Icelandic Institute of Nature Research, Garðabær, Iceland

[3] GFZ Helmholtz Centre for Geosciences, Potsdam, Germany

[4] Department of Geosciences, Dickinson College, Carlisle, PA, USA

[5] Acres of Ice, Ladakh, India

[6] School of Marine and Environmental Programs, University of New England, ME, Biddeford, USA

Published online: 06 June 2026

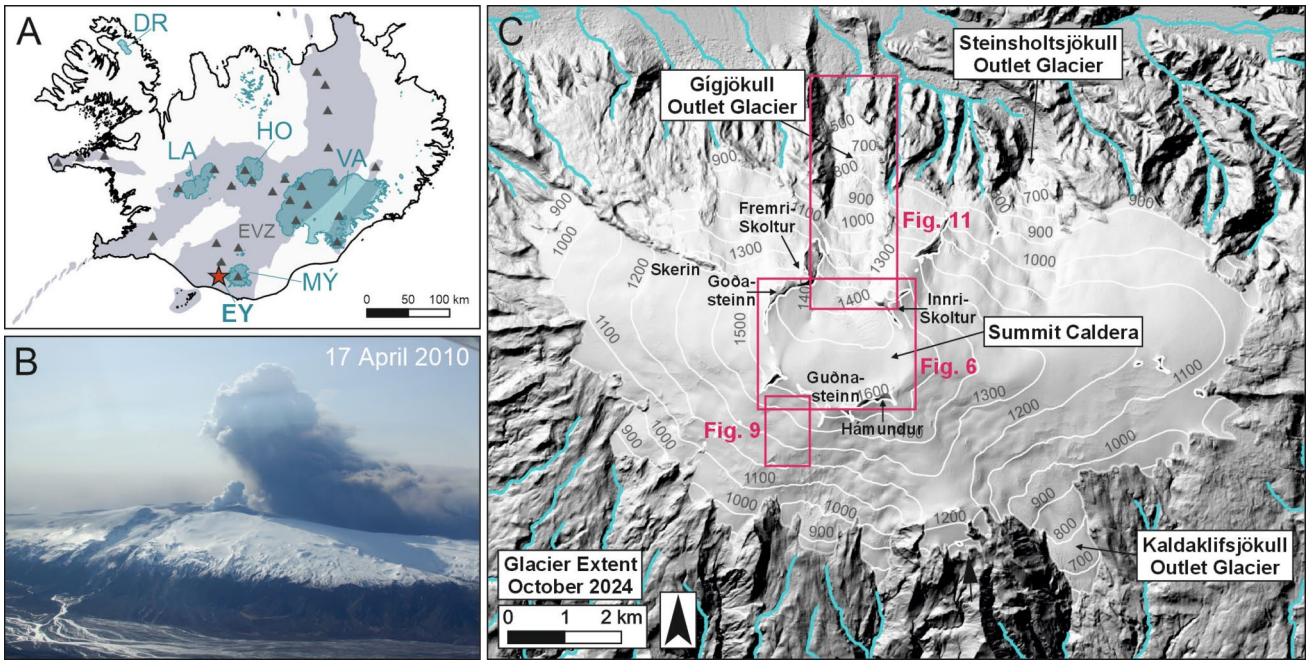

Fig. 1 Location of Eyjafjallajökull in Iceland and overview of the Eyjafjallajökull ice cap. **A** Map of Iceland with main volcanic zones (light gray) and central volcanoes (dark gray triangles) after Jakobsson et al. (2008). Glacier outlines (from 2019) derived from Hannesdóttir et al. (2020). VA = Vatnajökull, LA = Langjökull, HO = Hofsjökull, MÝ = Mýrdalsjökull, DR = Drangajökull, EY (red star) = Eyjafjallajökull. **B** Aerial photograph of Eyjafjallajökull and Gígjökull during the eruption; viewing direction is toward the south/southeast. Image taken on 17 April 2010. **C** The glacier-covered part of Eyjafjallajökull with main geomorphologic features, glacier extent as in October 2024 (modified after Hannesdóttir et al. 2020), and surrounding rivers (Landmælingar Íslands). Background digital elevation model (DEM): hillshade representation of Pléiades satellite imagery from 12 October 2024. Altitudes are in m a. s. l.

Eyjafjallajökull, for example, lost ~ 2.5 km^2 between 2019 and 2024 (Table 1). Glacier expansion occurred over several hundred years during the Little Ice Age (LIA), and the glaciers reached their maximum in the late nineteenth century. Strong mass loss was observed since then (ca. 1890). Taking into account the glacier development until 2019,

Table 1 Area and volume calculations for Eyjafjallajökull. Separate calculations were made for (i) the entire ice cap and (ii) the caldera and Gígjökull only (Gígjökull ice catchment). The difference between (i) and (ii) is indicated as well

Year	Area (km^2)	Time span	Volume change (m^3)	Average elevation change (m) for individual time spans	Average elevation change (m) per year	Uncertainty (m) per year
Eyjafjallajökull						
2010	72.25	2010–2014	-1.56×10^8	−2.20	−0.55	±0.25
2014	69.68	2014–2021	-1.51×10^8	−2.24	−0.32	±0.14
2021	65.09	2021–2024	-2.57×10^8	−3.90	−1.33	±0.33
2024	63.47	2010–2024	-5.64×10^8	−8.32	−0.59	±0.07
Caldera/Gígjökull (Gígjökull ice catchment)						
2010	6.86	2010–2014	$+1.28\times10^7$	+1.83	+0.46	±0.25
2014	7.15	2014–2021	$+7.38\times10^7$	+10.28	+1.47	±0.14
2021	7.21	2021–2024	$+7.93\times10^6$	+1.10	+0.37	±0.33
2024	7.27	2010–2024	$+9.45\times10^7$	+13.38	+0.96	±0.07
Eyjafjallajökull minus caldera/Gígjökull						
2010	65.39	2010–2014	-1.69×10^8	−2.64	−0.66	±0.25
2014	62.53	2014–2021	-2.25×10^8	−3.73	−0.53	±0.14
2021	57.88	2021–2024	-2.65×10^8	−4.63	−1.54	±0.33
2024	56.20	2010–2024	-6.59×10^8	−10.84	−0.77	±0.07

almost half of the total mass loss has occurred since 1994/95, corresponding to 240 ± 20 Gt or an average loss of 9.6 ± 0.8 Gt per year (Adalgeirsdóttir et al. 2020). Since no long-term changes in precipitation have been reported (which is different from the global trend), glacier retreat is considered mostly a result of climate warming and therefore high melting during the summer months. Precipitation in Iceland arrives with prevailing southerly winds with the highest amount on the southern slopes of Vatnajökull and Mýrdalsjökull. Annual precipitation exceeds 4000–5000 mm with peaks even reaching 7000 mm (Crochet 2007; Björnsson and Pálsson 2008). Glacial surges, common at the outlet glaciers of all the major ice caps in Iceland and observed over several centuries (historical reports), also significantly alter the geometry of glaciers and lead to thinning of the accumulation area and thickening of the glacier terminus (Björnsson 2017). Volcanic and geothermal activity can similarly contribute to glacier changes, although usually to a smaller extent and often on shorter time scales. While currently 60% of the ice caps in Iceland are underlain by active volcanoes or hydrothermal systems (Björnsson and Pálsson 2008), jökulhlaups are the most frequently occurring volcanic hazard (Gudmundsson et al. 2008). The interactions between volcanoes and glaciers have been studied in detail, resulting in a better understanding of glacier response to rapid melting of ice with various thicknesses (Magnússon et al. 2012). These include thin ice conditions (50–200 m) as observed at Grímsvötn (Reynolds et al. 2018), as well as much thicker ice (600–750 m) as existing above Gjálp (Jarosch et al. 2008). Other interactions with the cryosphere and relevant in Iceland include permafrost degradation, which could cause slope instability, or minor steam explosions (e.g., Askja) due to sudden release of pressure in the geothermal system (Shevchenko et al. 2024). Isostatic rebound is another effect of ice retreat and can lead to increased magma production in the shallow mantle due to reduced pressure and thus impact the behavior of volcanoes (Sigmundsson et al. 2010b).

Considerable volcano-ice interactions also characterized the first few days of the 2010 summit eruption of Eyjafjallajökull, lasting from 14 April to 22 May 2010 (Magnússon et al. 2012). The ice-capped Eyjafjallajökull volcano is located on the south coast of Iceland and belongs to the southern part of the Eastern Volcanic Zone (EVZ) (Fig. 1A). It is a relatively low-aspect ratio (east-west elongated) stratovolcano (Loughlin 2002) (Fig. 1B), which is located in direct proximity to Iceland's Ring Road and tourist attractions such as Seljalandsfoss and Þórsmörk. In 2024, 14 years after the eruption, the glacier covered an area of ~ 63.5 km^2 (Table 1). Main outlet glaciers are Gígjökull, draining from the summit caldera through a breach to the north, the nearby Steinsholtsjökull, and Kaldaklifsjökull in the southeast (Fig. 1C). The 2010 summit eruption, which quickly emerged through the ice cover after its start, caused rapid melting of ice and the formation of ice cauldrons (sinkholes in ice). Extensive jökulhlaups were observed during the first few days, propagating from the former existing proglacial lake Gígjökulslón on the north side of the volcano (Magnússon et al. 2012). Major disruption to European air traffic was caused by glacial meltwater-magma interaction causing fragmentation and an eruption plume reaching a height of nearly 10 km and significant ash dispersal toward the southeast in the first few days after eruption onset (Gudmundsson et al. 2010). In addition, a subglacial lava flow (later subaerial) emerged in the summit caldera and propagated down the Gígjökull outlet glacier (Oddsson et al. 2016b).

Eyjafjallajökull is tectonically connected to the nearby Katla volcanic system through east-west striking faults and eruptive fissures (Einarsson & Sæmundsson 1987). The volcanic edifice has been building over the last 800,000 years (Loughlin 2002) and is known as a relatively quiet volcano compared to its neighboring volcanoes Katla and Hekla (Gudmundsson 1996). Its only known eruptions in historic times prior to 2010 were in 920 CE (formation of the Skerin Ridge) (Óskarsson 2009; Larsen 2000), 1612, and 1821–1823 (Thoroddsen 1925). The edifice then remained seismically quiet until 1991. Intense seismic swarms in 1994, 1996, and 1999–2000 delineated pathways of magma intrusions into the volcano (Hjaltadóttir et al. 2009), escorted by intense deformation (Pedersen and Sigmundsson 2004; Sturkell et al. 2010), before finally culminating in another eruption period lasting from March to May 2010. Deformation studies by Sigmundsson et al. (2010a) suggested that multiple storage regions existed and deformation did not only relate to a single magma chamber. Starting as a flank eruption at Fimmvörðuháls in the east (Edwards et al. 2012), activity eventually shifted to the summit caldera and substantially impacted the overlying ice cap (Magnusson et al., 2012; Oddson et al. 2016b).

The volcano is characterized by a 2–3 km wide summit caldera with several nunataks indicating the caldera rim (Fig. 1C). Ice thicknesses varied from ~ 200 m in the western part of the caldera (Strachan 2001) (pre-eruption conditions) up to ~ 400 m in the eastern part (May 2011), as unpublished data collected by the Institute of Earth Sciences (University of Iceland) revealed. Magnússon et al. (2012) estimated a total (pre-eruption) ice volume of ~ 0.8 km^3. The volcanic flanks have thinner ice, typically less than 150 m (Loughlin 2002; Strachan 2001). In 2024, glacier termini of the volcano's main outlet glaciers were found at elevations ranging from ca. 500 (Gígjökull) to 600 m a. s. l. (Kaldaklifsjökull, Steinsholtsjökull) (Fig. 1C).

While the eruption in 2010 received substantial scientific attention, including detailed studies of plume dynamics, volcanic ash, and the immediate impacts on the glacier cover and related hazards (e.g., Woodhouse et al. (2013), Ripepe

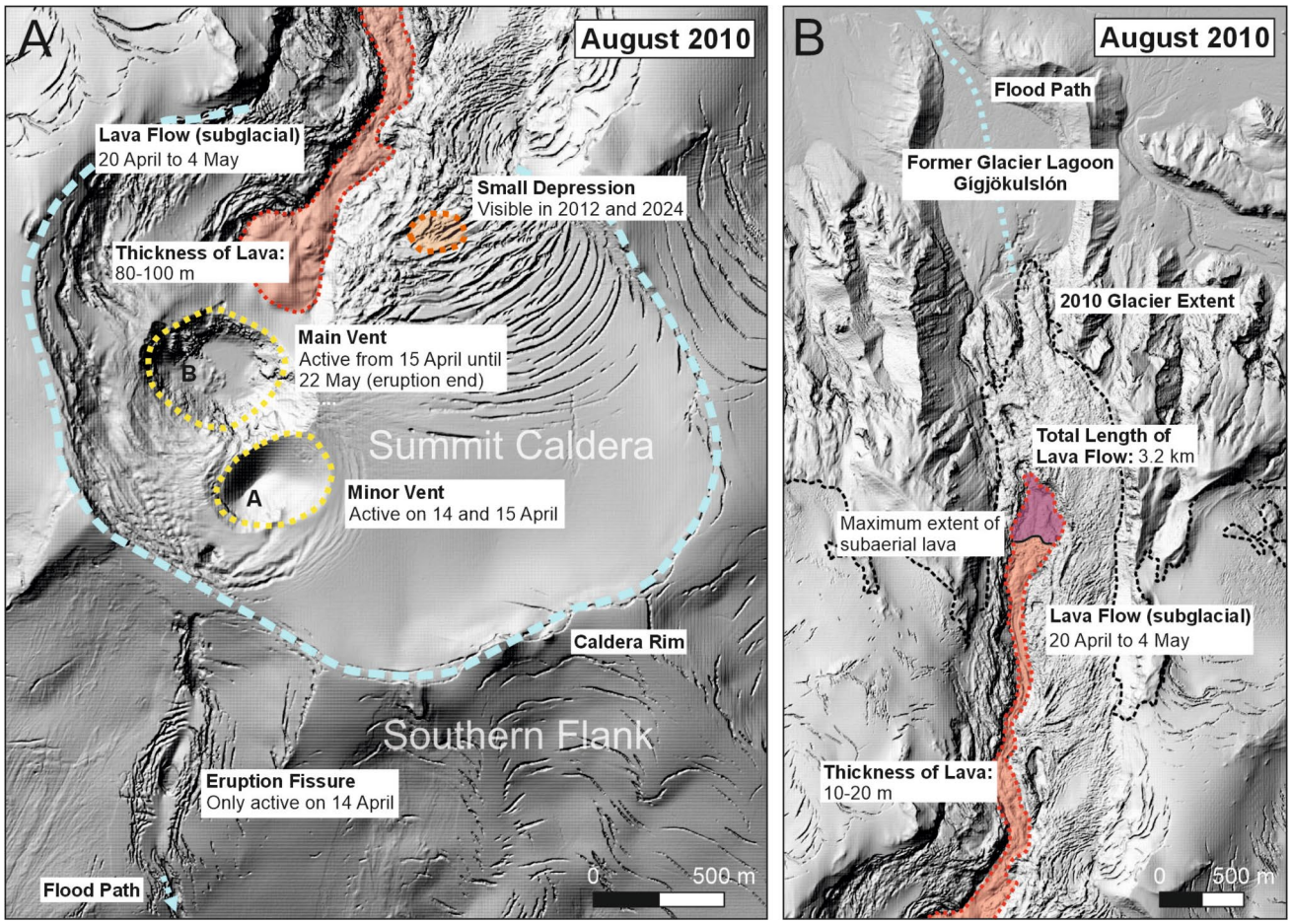

Fig. 2 State of Eyjafjallajökull (summit area and Gígjökull) in August 2010—almost 3 months after the end of the eruption. Hillshade representation of a LiDAR DEM from Jóhannesson et al. (2013). Locations, extent of eruption structures, and related information derived from Magnússon et al. (2012) and Oddsson et al. (2016b). **A** Summit caldera with parts of the southern flank and the upper part of the outlet glacier Gígjökull to the north. Capital letters A and B (minor and main vent) correspond to the cauldrons described in Magnússon et al. (2012). The southern cauldron (A) formed in the first 2 days of the eruption; the northern cauldron (B) developed on the second day and merged with a pre-existing one formed on the first day of the eruption. Location of a small cauldron is visible on aerial photographs taken from an airplane in September 2012 and October 2024. **B** Gígjökull outlet glacier with lava path, 2010 glacier extent (post-eruption) and former glacier lagoon Gígjökulslón. Purple color represents the maximum extent of (initially) subglacial lava; red color indicates the maximum extent of subaerial lava on top of the initially subglacial lava. Glacier outline was modified after Hannesdóttir et al. (2020)

et al. (2013), Spinetti et al. (2013), Dürig et al. (2022)), there has been no systematic analysis of the post-eruption evolution and glacier recovery. During the eruption, three different areas of the glacier were affected. (i) The summit caldera: Activity initially started on a short N-S trending fissure, forming two individual cauldrons during eruption onset. A third cauldron became visible on the second day but merged with the initial (first day) northern cauldron and eventually became the main vent. Activity continued for almost 6 weeks. Lava accumulation, starting on 20 April, also impacted the ice in the caldera. (ii) The southern flank: A short-lived (1 day) eruption fissure evolved on the first day in the upper part of the flank close to the caldera rim. (iii) The outlet glacier Gígjökull: (Subglacial) lava propagation over more than 2 weeks melted substantial parts of the outlet glacier. Lava accumulation started subglacially in the caldera and eventually became subaerial while progressing northwards, finally reaching a length of more than 3 km. After the ice was melted, another subaerial lava flow was emplaced on top of it, forming a 2.7-km long a'a lava field. An overview of the immediate eruption impacts, described in detail by Magnusson et al. (2012) and Oddsson et al. (2016b), is shown in Fig. 2 and is needed for the further understanding of the paper and discussion of specific areas.

Here, we study how the ice cap has evolved after the eruption and how individual areas have changed with time. We use elevation data obtained from Pléiades, SPOT5, and LiDAR scans to calculate elevation and volume changes over

varying time periods between 2008 and 2024, illustrate the changes in glacier extent, and investigate the complex ways of material gain, loss, and redistribution. Aerial photographs and on-site investigations help to illustrate visual changes through time and space. These data allow us to (i) identify the long-term impacts of individual eruption stages on specific areas of the ice cap, (ii) compare these areas to the development of the ice cap as a whole, and (iii) characterize the current state of the volcano and glacier. Since glaciers globally are retreating at an alarming rate, it is essential to understand the long-term impacts of eruptions on their dynamics and recovery. Furthermore, changes of the ice cover can often serve as precursors for renewed activity and long-term studies can thus help to respond faster to changes in volcanic activity and related hazards.

Data and methods

Data

Data used for this study can be divided into three different groups. The first group comprises photographic material from various overflights and on-site investigations before, during, and after the eruption. Details about the photographs (e.g., viewing directions and date) are provided in the respective figure captions or in the appendix. The second group consists of different elevation data both airborne and satellite-based. Data from July 2008 derive from SPOT5 and have a resolution of 10 m. The August 2010 airborne LiDAR DEM was published by Jóhannesson et al. (2013) and has a resolution of 2 m. Data sets from August 2014, September 2021, and October 2024 were obtained from Pléiades and all have a resolution of 2 m. The satellite-born data (SPOT5 and Pléiades) are pushbroom stereo images, whereby particularly the Pléiades stereo images allow for a processing of highly accurate elevation models (Berthier et al. 2014). The 2010 LiDAR DEM is part of an airborne LiDAR campaign carried out between 2008 and 2012, surveying the main glaciated regions in Iceland. These data are characterized by a high resolution with submeter uncertainties (Jóhannesson et al. 2013). Details about the processing of respective data sets are provided by Belart et al. (2019). The last data group comprises information about varying glacier extents from a glacier inventory by Hannesdóttir et al. (2020) (ongoing work), Belart et al. (2020), and Jöklavefsjá. Some of the data here were slightly modified where the DEM difference clearly revealed a slightly different position of the glacier margin. This could either be elevation gain at the front of an advancing glacier, where the DEM difference reveals the position of the glacier front corresponding to the latter DEM, or elevation loss at the front of a retreating glacier, where the DEM difference reveals the position of the glacier front corresponding to the former DEM. The following glacier margins were used for this study: 2000–2003, 2010, 2014, 2019, 2021, and 2023. Modifications were made for 2010, 2014, and 2021. The 2023 extent was used to infer the 2024 extent, as only minor changes between these years were visible.

Data processing

The aim of the data processing was to create different time series with the various photographs and visualize changes of the ice cap through the years, calculate volume and elevation changes, and illustrate/calculate the variations in glacier extent. While the photographs were only used for visual documentation and did not go through a specific processing, details about the processing of elevation data are specified below. Preprocessing (e.g., alignment of data) was done as described by Belart et al. (2019) and is not further discussed in this work.

Elevation changes between individual DEMs were calculated in QGIS (version 3.38.3) using the "Raster Calculator" and subtracting respective data sets; e.g., LiDAR DEM 2010 minus SPOT5 2008 represents the elevation change from 2008 to 2010. For a better comparison of the overall ice cap, elevation changes were calculated per year, meaning that the calculated difference was divided by the number of years between individual surveys. Elevation changes of specific areas impacted by the eruption (caldera, Gígjökull, southern flank) were calculated for individual time spans and not per year. For these areas, minor gaps in the subtracted DEMs were interpolated using the "Fill NoData" tool in QGIS. Finally, contour lines showing the elevation changes were extracted from the respective DEMs. For the overall glacier area, contour lines indicate the real elevation of the glacier (in m a. s. l.) as in August 2014, September 2021, and October 2024. In addition, different glacier extents were added.

Elevation information for individual profiles was extracted in two different ways. Elevation profiles for Gígjökull were extracted from the respective data sets via the "Terrain Profile" tool in QGIS. The elevation profiles of the caldera were extracted via the "Residuals Function" in Surfer 13.

To accurately obtain volume changes integrated from the DEM difference, some initial steps were necessary, including gap interpolation in the data sets and the determination of the maximum glacier margins for individual time spans. The DEMs we used for this study had various gaps varying in size and location. Before subtracting the DEMs, gaps outside the glacier margins were replaced with data from the 2024 Pléiades DEM, since the elevation in ice-free areas should be the same for all years. This reduced in particular the data gap on the southwest side of the glacier in 2014. Gap interpolation was then done in the subtracted

DEMs with a two-step filtering. First, with the Gaussian 13 pixel × 13 pixel filter (26 m × 26 m) to eliminate smaller data gaps. Second, a 260 m × 260 m median filtering to deal with larger gaps. Then, the different layers were mosaiced: (a) unfiltered subtracted DEMs, (b) Gaussian filtered subtracted DEMs, and (c) median filtered subtracted DEMs in such a way that (a) was used where data already existed, (b) was used where (a) had gaps, or (c) was taken where (a) and (b) had gaps. With this approach, all data gaps could be filled except for the 1.16 km^2 gap in the subtracted 2010–2014 DEM and the 1.35 km^2 gap in the subtracted 2014–2021 DEM on the southwest side. Here, we took a look at the average lowering in the surrounding areas at a similar elevation for the two periods and assumed average lowering also applied to the missing area. This resulted in 8.8-m estimated lowering for these gaps in the 2010–2014 period and 7.0-m lowering for 2014–2021. The maximum glacier extent for the respective time periods was inferred from the DEM difference. Finally, we calculated the average lowering of the ice cap per year taking into account the area at the start and the end of each time period (mean) and the numbers of years each period has. All calculations were done in MATLAB (Version R2023b).

For errors contributing to the uncertainty of the calculated volumes, we assume ± 1 m as possible bias in elevation change maps relative to the 2024 DEM of Eyjafjallajökull. This can be considered a generous estimate compared to geostatistical uncertainty estimates for similar datasets such as discussed by Magnússon et al. (2016) and Belart et al. (2020).

Results

Development of the overall ice cap

For comparison between the different time spans, we normalized elevation changes to 1 year. Focus here is the ice cap overall; elevation changes for the areas impacted by the eruption will be discussed in detail in "The summit caldera," "The southern flank eruption fissure," and "The outlet glacier Gígjökull."

Results show major elevation changes occurring in the center (eruption impacts) and along the margins of the ice cap. The ice cap overall is shrinking. This can be seen in the elevation change maps (Fig. 3), the volumetric changes, and the glacier extent (Table 1). Elevation change maps reveal that the greatest annual elevation loss at the glacier margins happened between September 2021 and October 2024, followed by the period from August 2010 to August 2014. Less elevation loss occurred between August 2014 and September 2021. Annual values mostly ranged between 0 and −6 m, although significantly greater loss was visible at the outlet glaciers. Between August 2010 and September 2014, Steinsholtsjökull revealed annual elevation losses of up to 20 m (Fig. 3A). The outlet glacier substantially thinned in the following periods and revealed a strong retreat. Although loss dominated the glacier margins from 2010 to 2014, slightly positive values (0–1 m) were observed over large parts on the eastern and southern flanks. Some areas with elevation gain also existed from 2014 to 2021 (Fig. 3B). Compared to the first two time spans (August 2010 to August 2014 and August 2014 to September 2021), much stronger elevation loss happened from 2021 to 2024 with annual changes between −1 and −2 m at elevations up to 1300 m (Fig. 3C). A slight elevation gain was only visible at the southeastern flank. All glacier margins showed a clear thinning, specifically visible at Kaldaklifsjökull and Steinsholtsjökull.

From 2010 to 2024, a constant retreat of the ice cap was observed (Table 1). The area shrunk from 72.3 to 63.5 km^2 with substantial volume loss, corresponding to an average lowering of ~ 8.3 m over that time span. However, although the ice cap overall revealed significant area, volume, and elevation losses, the opposite was observed at the caldera and Gígjökull. Over the entire period from 2010 to 2024, these areas had a positive mass balance with significant volume increase between 2014 and 2021 (7.38×10^7 m^3, average gain of ~ 10.3 m). Overall, an average elevation gain of ~ 13.4 m was calculated for the entire time. The calculated numbers indicate that the caldera and Gígjökull behaved differently than the rest of the ice cap and the volume increase in these areas reduced the overall loss of the ice cap.

The summit caldera

The eruption significantly changed the area of the summit caldera as a direct comparison between photographs from October 2004 (pre-eruption) and June 2010 (almost 1 month after the eruption) reveals (Fig. 4). The dimensions became clearly visible toward the end of the eruption and were documented in detail during the first few years after the eruption (May 2010 to October 2013). One day before the eruption ended (21 May 2010), the caldera was characterized by two vents with only the main vent showing activity (Fig. 5A). In addition, the extent of initially subglacially emplaced lava in the northern part of the caldera became obvious. In June 2010, almost 3 weeks after the eruption ended, steam emission dominated from the main vent, although emanations were also visible from the lava. Tephra covered major parts of the caldera and large parts of the upper volcanic flanks (Figs. 4 and 5B). A lake, visible in aerial images from July 2010, had formed in the main vent and filled its entire bottom (Fig. 5C). It remained at least until August 2011, even though it had largely shrunk by that time. In July 2011, 420 days after the end of the eruption, tephra accumulations in the caldera were mostly covered by snow again. Large

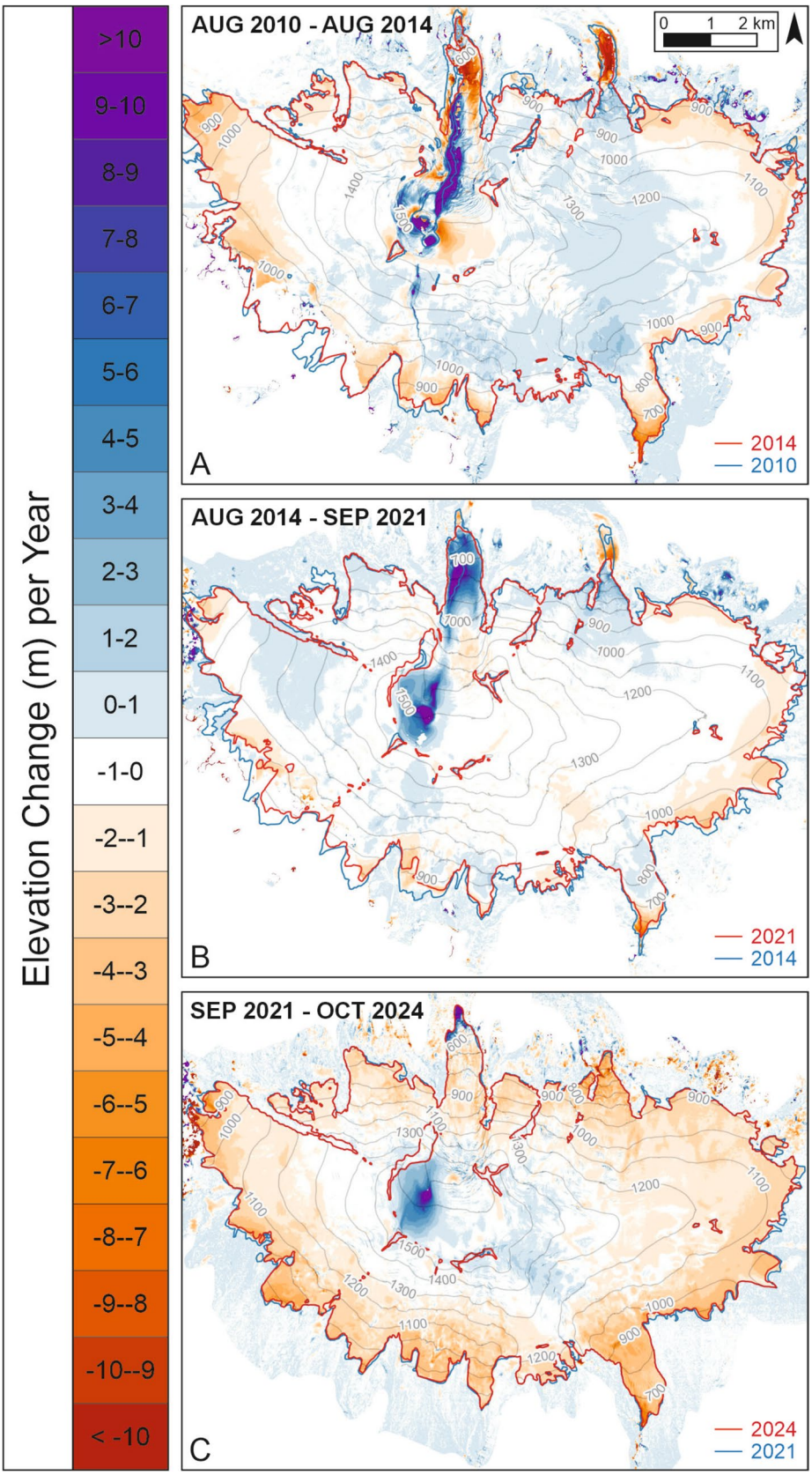

Fig. 3 Annual elevation changes (m) of the Eyjafjallajökull ice cap over three different time periods. Note: Areas impacted by the eruption and Steinsholtsjökull (up to ± 20 m change) exceed color scale. See Figs. 6, 9, and 11 for details. **A** August 2010 to August 2014. **B** August 2014 to September 2021. **C** September 2021 to October 2024. Isopaches (100-m interval) with numbers indicate elevations in m a. s. l.

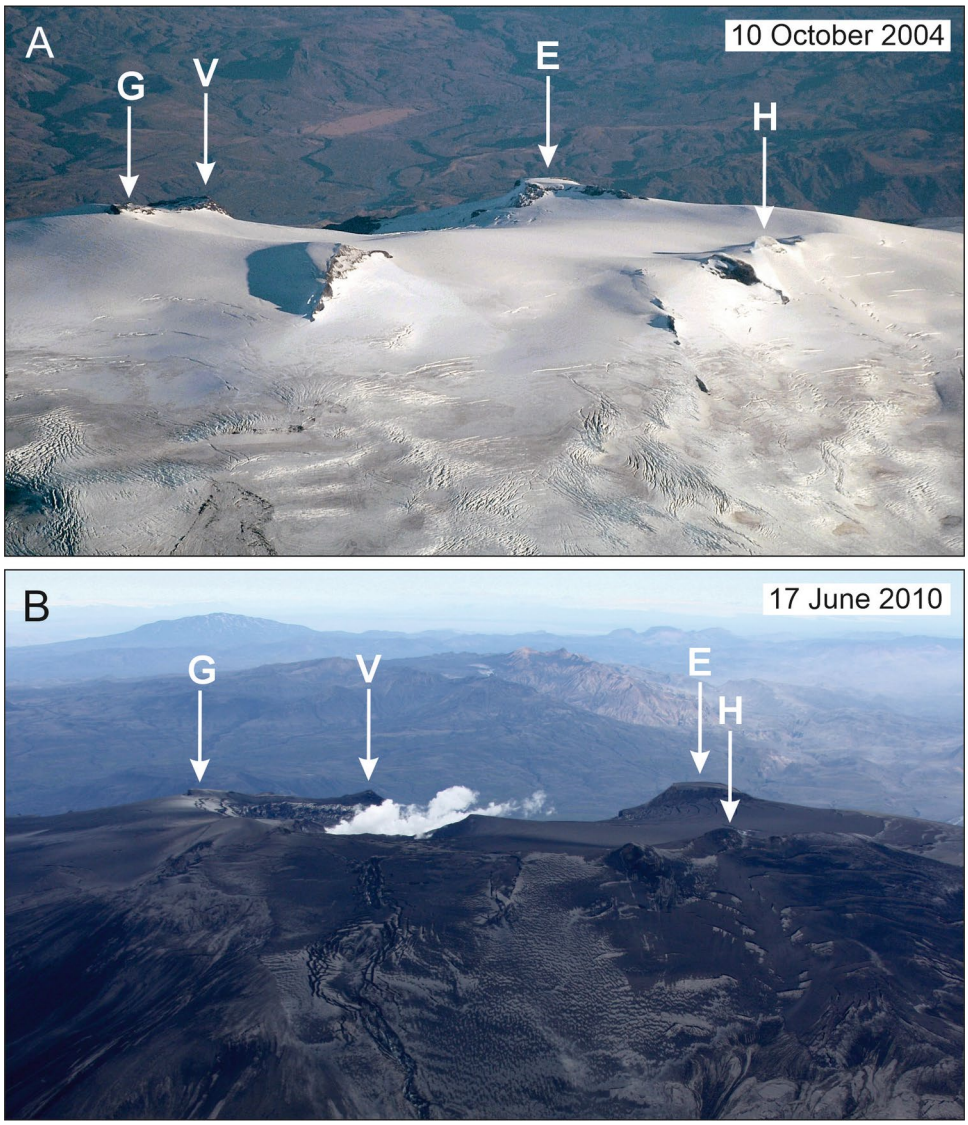

Fig. 4 The summit of Eyjafjallajökull before and after the eruption. **A** 10 October 2004; almost 6 years before the eruption; view from SSW. **B** 17 June 2010; covered by thick tephra after the eruption; view from SSW. G: Goðasteinn; V: Vestari Skoltur; E: Eystri Skoltur, and H: Hámundur. The width of the summit caldera (east-west) is 2.5 km. The photographs were taken from an airplane

parts of the minor vent had refilled and only a depression was left, which indicated its initial position adjacent to the main vent toward the southeast. The main vent and the lava pile, however, were still visible. While the main vent already revealed some snow accumulations at the bottom and the lake had mostly vanished, the lava remained completely exposed (Fig. 5D). An aerial image from September 2012 reveals that the eruption structures as described before were still apparent, although more snow has accumulated on top (including the lava). Clear steaming could be noticed from the eruption deposits confining the northern rim of the main vent. In contrast to observations in 2010 and 2011, a new depression in the northern part of the caldera first became visible in September 2012 (Fig. 5E). Further refilling of the main vent took place until October 2013 with snow mostly sliding down over its southern rim. Minor steam emissions were still visible on the northern rim (Fig. 5F). The new depression remained visible until at least October 2013 as seen in different aerial images from that time. A small cavity visible just east of the main vent is also conspicuous (Fig. 5F).

During the eruption, considerable morphology changes took place in the caldera. These changes are not only visible in aerial photographs (Figs. 4 and 5) but also in different types of elevation data. Figure 6 illustrates the visual development of the caldera from 2010 (post-eruption) to 2024 as revealed by LiDAR and Pléiades data (upper gray hillshade images). A comparison of images resulted in three key observations: (i) The glacier recovered and most of the visible eruption impacts have vanished completely by 2024; (ii) the recovery time of individual areas varies; the fastest recovery was visible in the area of the minor (southern) vent, followed by the main (northern) vent; the longest recovery time was observed in the area

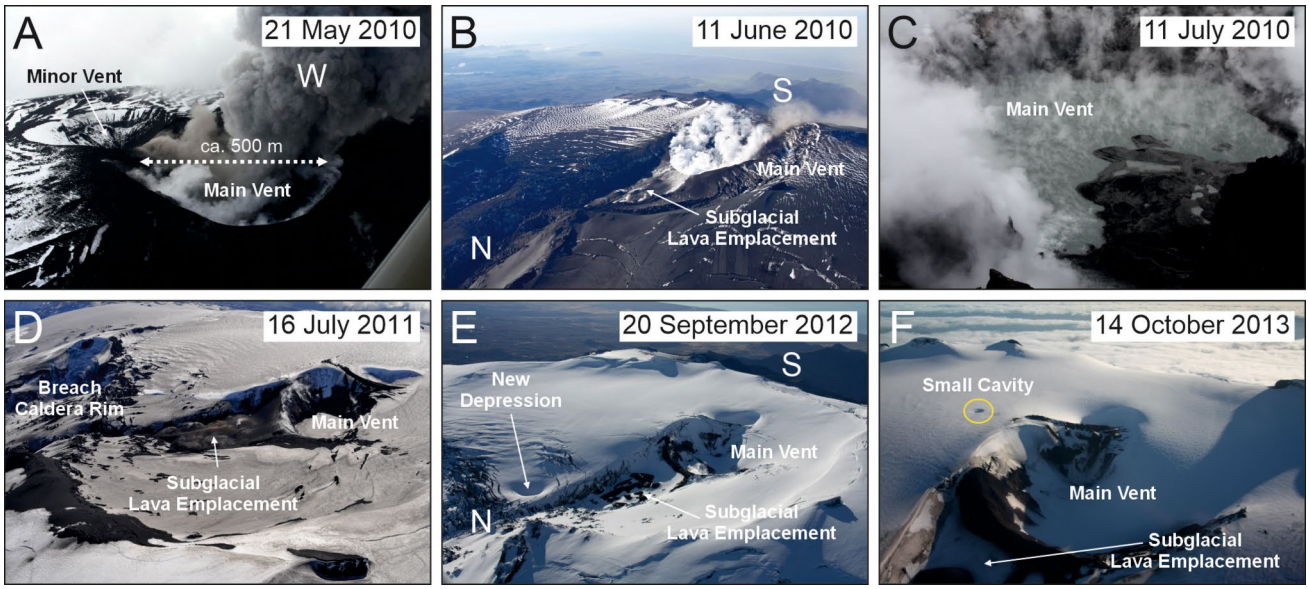

Fig. 5 Visual development of the summit caldera based on aerial photographs taken from an airplane. **A–F** Development of the summit caldera with vent areas and subglacial lava from 21 May 2010 to 14 October 2013. Further details are provided in Appendix A

of lava accumulation; and (iii) the most notable changes took place in the first few years after the eruption, mainly from 2010 to 2014, and then from 2014 to 2021. The morphology of the glacier surface did not significantly change from 2021 to 2024.

A comparison of the glacier surface elevation between August 2008 and August 2010 reveals the immediate eruption impact on the summit area. While the eastern half and areas close to the caldera slightly gained in mass (10 m maximum), considerable loss occurred in the western half with a maximum surface lowering of −160 m. The area of the main vent had the largest elevation change, −120 to −160 m within a diameter of ca. 250 m. The elevation change in the area of lava accumulation ranged between −80 and −120 m and up to −120 m in the center of the southern vent, which was only active in the first days of the eruption (Fig. 6A). The post-eruption time between 2010 and 2014 reveals a reverse situation. The ice cauldrons (vents) started to fill up, with positive elevation changes reaching 80 m. The areas adjacent to the vents, both on the east and west sides, showed elevation loss of up to −20 m (Fig. 6B). The following two periods from 2014 to 2021 and from 2021 to 2024 show a similar pattern with elevation loss in the eastern half of the caldera and gain in the west. While the greatest mass accumulation between 2014 and 2021 occurred in the area of the main vent (up to 90 m), followed by the area impacted by lava (Fig. 6C), no elevation changes exceeding 10 m were observed in the vent areas in the period 2021 to 2024. However, two areas within the caldera stand out in comparison to their surroundings: first, a circular area with −10 m loss in the northern part of the caldera close to the breach, and second, the area of lava accumulation which rose by up to 40 m (Fig. 6D).

Appendix B illustrates the overall post-eruption elevation changes from 2010 to 2024. The elevation difference between August 2010 and October 2024 summarizes the total changes since 2010 and illustrates the elevation loss/gain for different segments. Overall, the comparison reveals how the area is recovering due to the strong positive mass balance at this high elevation.

Individual cross sections of the minor and main vent as well as a rough outline of the post-eruption bedrock topography are illustrated in Fig. 7. The southern, smaller vent quickly started refilling with snow after the eruption ended and already revealed a smooth surface in 2014. The initial vent structure had vanished completely by that time. In 2024, after constantly gaining mass, the area revealed a similar elevation level (slightly more) to the eastern part of the caldera (Fig. 7A). The main vent also started refilling after the eruption and large parts of the vent area were covered by snow again in 2014. However, the initial vent structure remained visible. Although an almost smooth surface was reached by 2021, the area still revealed the location of the vent center indicated by the funnel-like form of the depression. Similar to the minor vent, the surface level in 2024 was comparable to the eastern caldera section (Fig. 7B). Visible in both cross sections is the east-west bisection of the caldera, revealed by the bedrock topography (much deeper in the east) and partially indicated by the glacier surface. While the western part of the caldera constantly gained in mass after the eruption, the eastern part lost elevation and the 2024 surface is lower than the previous years illustrated in Fig. 7.

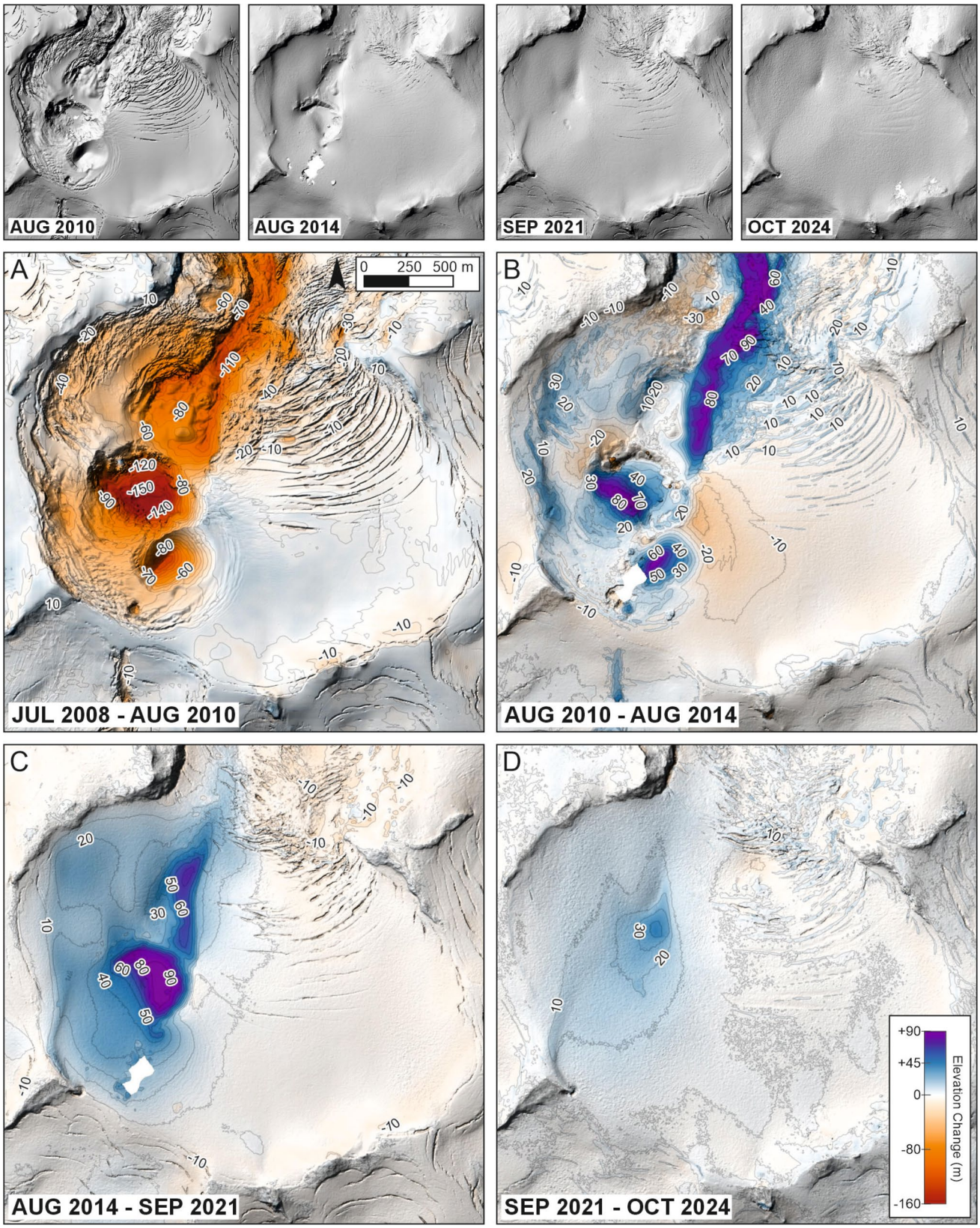

Fig. 6 Morphology of the summit caldera in individual years (upper grey hillshade images) and elevation changes (m) over four different time periods. **A** July 2008 to August 2010. **B** August 2010 to August 2014. **C** August 2014 to September 2021. **D** September 2021 to October 2024. Isopaches (10-m interval) with numbers indicate elevation changes

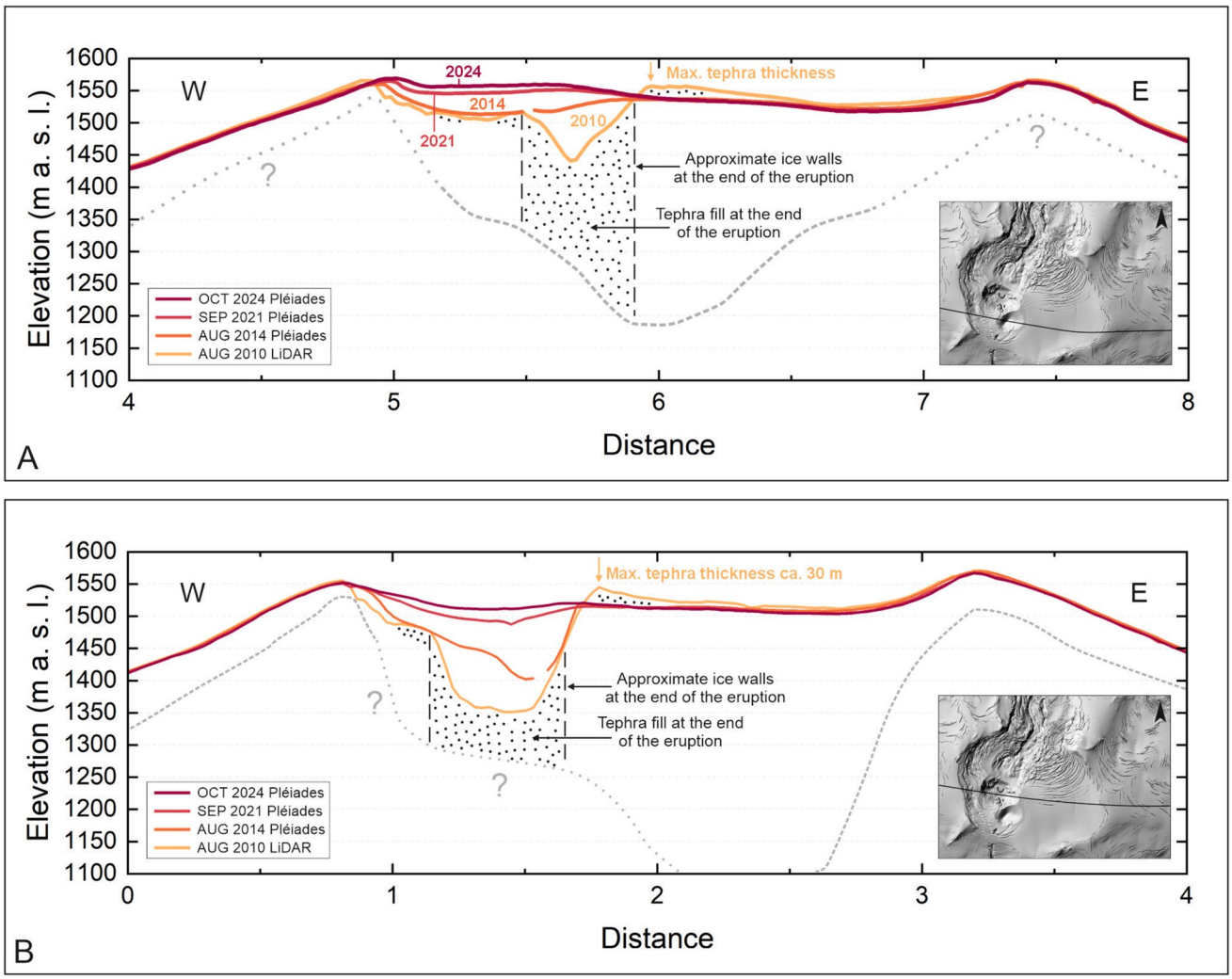

Fig. 7 Cross sections of the summit caldera (minor and main vent) with a rough outline of the post-eruption bedrock based on preliminary interpretation of ice penetrating radar profiles acquired within the caldera; unpublished data collected by the Institute of Earth Sciences (University of Iceland)

The southern flank eruption fissure

No visible heat output from the eruption fissure on the southern flank was evident by the end of April 2010, although the eruption in the caldera was still ongoing. Photographs even reveal that snow already started to accumulate on top of the fissure (Fig. 8A). While the southern flank was mostly covered by snow by the end of April and only minor patches of tephra were visible, the coverage had significantly increased by June 2010, where only little snow was visible (Fig. 8B). In September 2012, large parts of the fissure were buried under snow, although a cavity in the center of the fissure was still visible (Fig. 8C).

Elevation change calculations were also done for the southern flank eruption fissure (Fig. 9). Although the fissure on the southern flank was only active for one day during the eruption, some areas lowered by up to −60 m. The fissure is clearly visible on post-eruption LiDAR data from August 2010. Elevation loss was concentrated in two areas, visible as small circular depressions with elevation reductions between −30 and −60 m. Surrounding areas mostly reduced in elevation by −10 to −20 m; the flow path of the meltwater is visible as a narrow channel south of the eruption fissure progressing down the flank (Fig. 9A). Between 2010 and 2014, the glacier area impacted by the eruption nearly recovered completely and the loss observed from 2008 to 2010 had mostly been balanced. Surrounding areas, however, revealed an elevation reduction of up to −10 m (Fig. 9B). The area impacted by the eruption showed subtle elevation increase, by up to 5 m, between 2014 and 2021 (Fig. 9C), whereas the time period from 2021 to 2024 revealed elevation reduction,

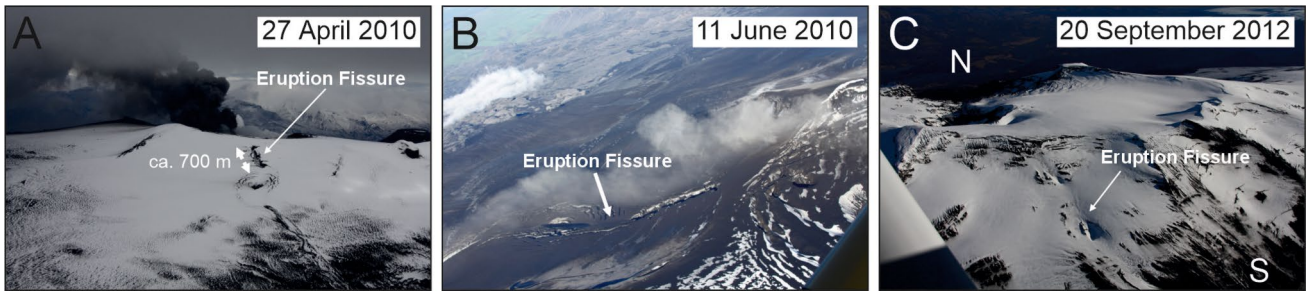

Fig. 8 Visual development of the southern flank based on aerial photographs taken from an airplane. **A–C** Development of the southern flank eruption fissure from 27 April 2010 to 20 September 2012. Further details are provided in Appendix A

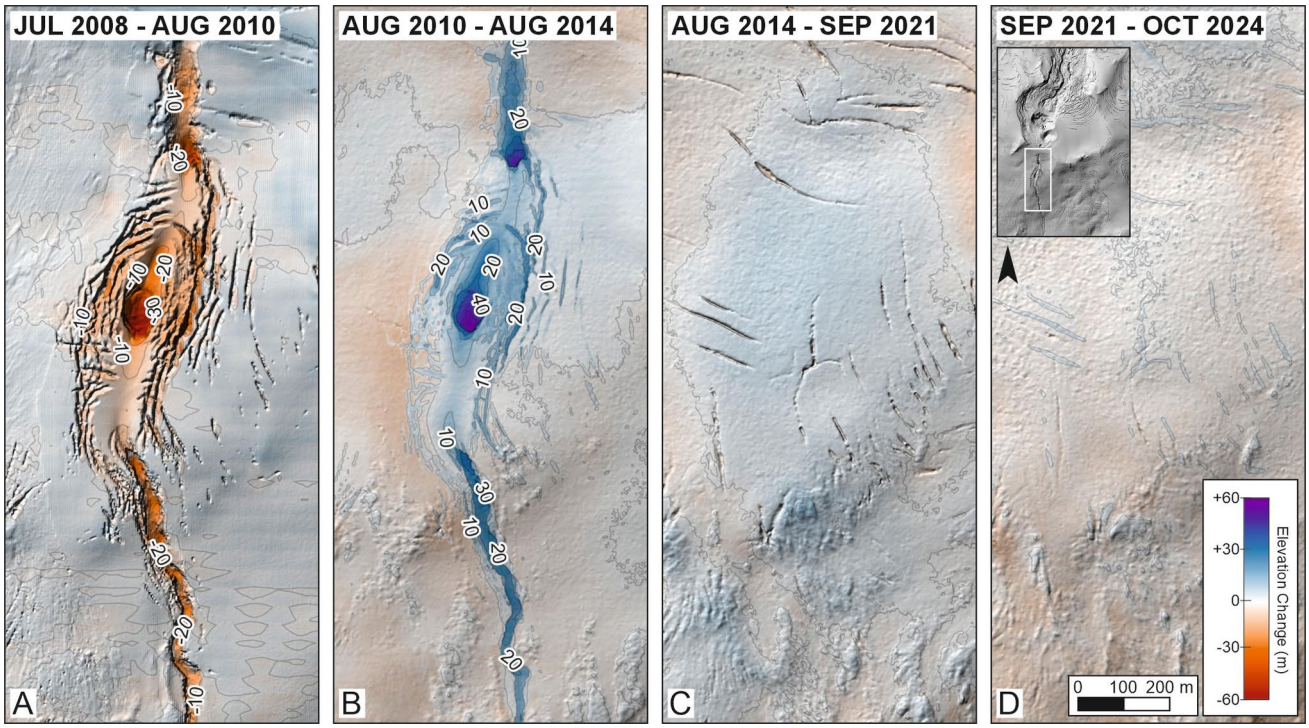

Fig. 9 Elevation changes (m) of the eruption fissure on the southern flank over four different time periods. **A** July 2008 to August 2010. **B** August 2010 to August 2014. **C** August 2014 to September 2021. **D** September 2021 to October 2024. Isopaches (10-m interval) with numbers indicate elevation changes

except for crevasses. Signs of the eruption had vanished completely by that time (Fig. 9D).

The outlet glacier Gígjökull

Post-eruption glacier outlines from individual years between 2014 and 2023 as well as photographs from March 2010 to September 2024 reveal the dynamics of Gígjökull's glacier terminus (Fig. 10). While retreat was observed from 2014 to at least 2017, the terminus advanced after that time period. In 2023, the terminus almost reached the 2014 glacier extent. The ice mass also expanded laterally, covering a larger area than in 2014. The shape of the terminus changed considerably, primarily the western section, but then remained mostly the same while advancing. The Gígjökull ice catchment increased in area from 6.86 km^2 in 2010 to 7.27 km^2 in 2024. While a retreat of the glacier terminus is visible from 2010 to 2014 (−150 m) and from 2014 to 2021 (−370 m), the glacier readvanced from 2021 to 2024 (+270 m). Photographs of Gígjökull taken between 2010 and 2024 also document the dynamics of the glacier terminus. Retreat is evident between 2010 and 2017, followed by a stagnation of the terminus position in 2017, with little or no ice from above reaching the lower parts. Readvance is then visible in 2024 again. The general topography of the area as shown in an aerial image from 2012 explains the

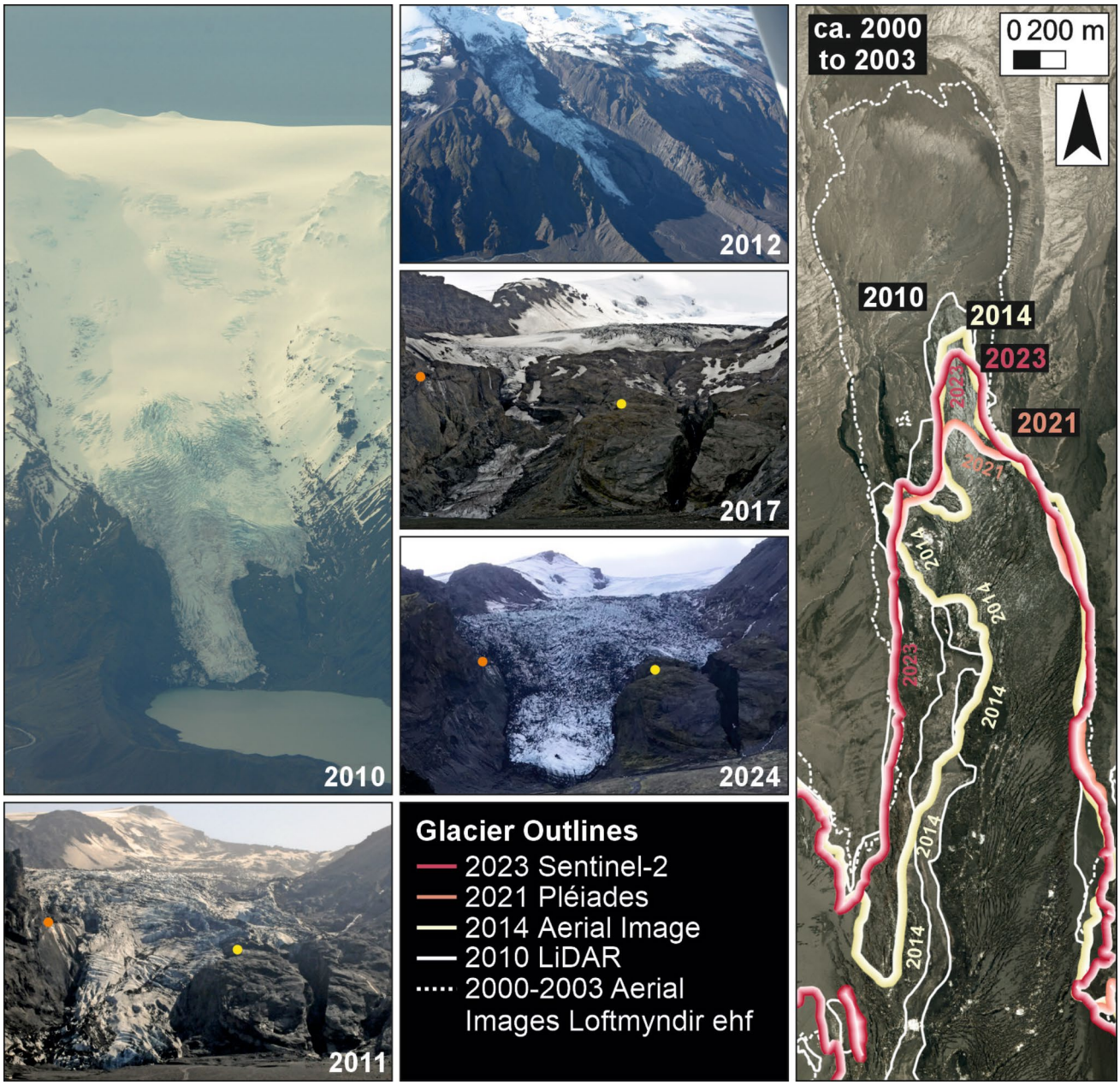

Fig. 10 Changes of the Gígjökull glacier terminus. Left: Images of the glacier front in 2010 (pre-summit eruption), 2011, 2017, and 2024. Yellow and orange dots are for reference and indicate the same locations on each image. An overview of the complete outlet glacier is shown for 2012. Right: Position of the glacier terminus during different years between 2000 and 2023. Background = aerial image (orthophoto) from July 2010 (Samsýn/Blom)

specific shape of the terminus which is confined by the uneven and prominent bedrock to the west. The lateral moraines are an additional indicator for the large extent of the outlet glacier in the past. Between ~ 2000 and 2003, the lateral glacier extent was confined by these moraines. Outlines from ca. 2000 to 2003 and 2010 (after the eruption) reveal that the glacier terminus did not reach the extent it had prior to the eruption. However, the photograph from March indicates only minor front changes during the eruption. The reduced glacier extent caused by the eruption was almost entirely caused by the lava emplacement further up-glacier. After some post-eruption phases of retreat, Gígjökull readvanced and its extent in 2024 nearly reached the terminus position from August 2010, 3 months after the end of the eruption.

Figure 11 represents the elevation changes of Gígjökull for different time periods between August 2008 and October 2024. Comparing the elevation difference between 2008 and 2010, a deep ice canyon with depths of −120 m

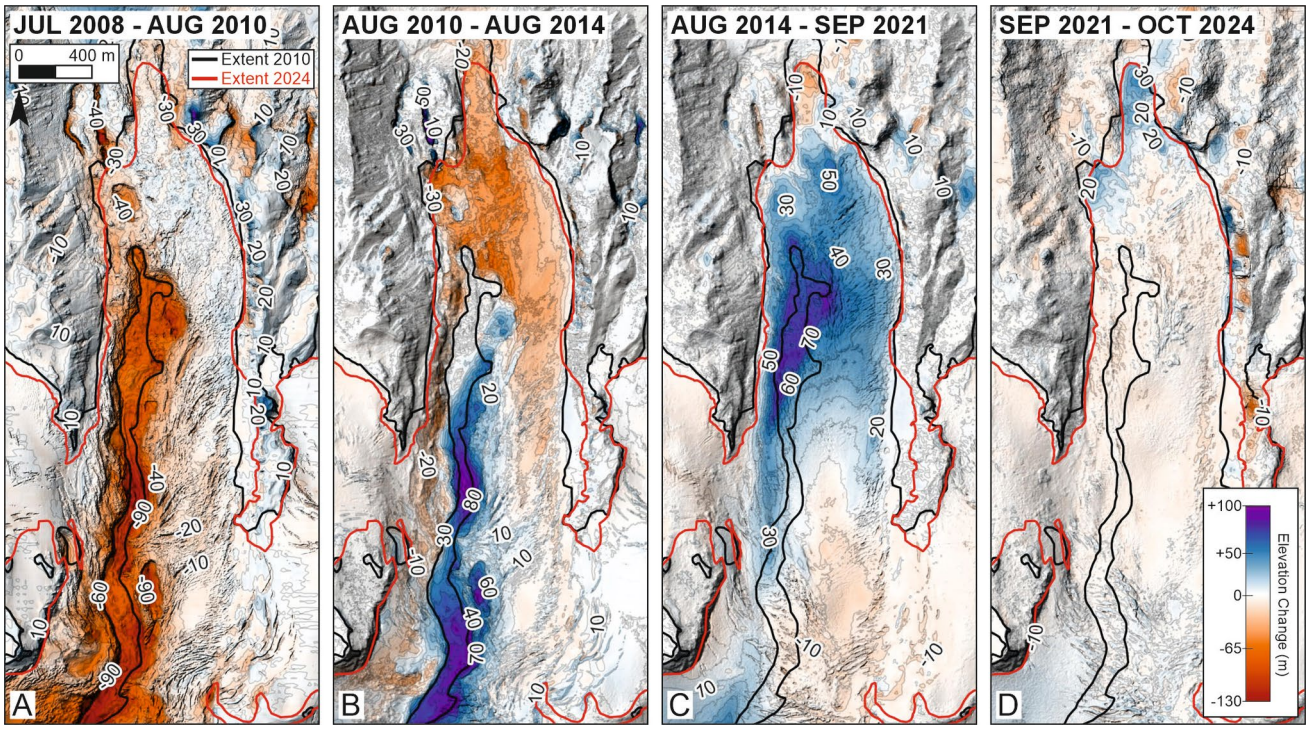

Fig. 11 Elevation changes (m) of the outlet glacier Gígjökull over four different time periods. Black solid line indicates the glacier extent in 2010; red solid line the extent in 2024. **A** July 2008 to August 2010. **B** August 2010 to August 2014. **C** August 2014 to September 2021. **D** September 2021 to October 2024. Isopaches (10-m interval) with numbers indicate elevation changes

becomes visible. The canyon was formed during the eruption by the lava flow, which emerged in the summit caldera. Although the lava initially expanded subglacially, it eventually melted the ice and became subaerial. In addition to the canyon formation, large parts of the glacier terminus significantly decreased in elevation, by up to −60 m (Fig. 11A). While refilling of the ice canyon and accumulation on top of the lava took place between 2010 and 2014, with maximum elevation increase of up to 80 m, the lower parts toward the glacier terminus and some areas close to the lava flow to the east experienced an elevation decrease of −40 to −60 m (Fig. 11B). The time period between 2014 and 2021 is different. Although an elevation increase through snow accumulation on the upper part of the lava (located in the caldera) was visible, only minor changes occurred in the middle part. Significant accumulation, however, took place at lower elevations, which previously experienced mass loss. As revealed by Fig. 11A, B, the lava flow was completely covered by glacier ice by 2021, evident through substantial elevation increase between 2010 and 2021. Close to its lower end, the glacier thickened by up to 80 m. An elevation decrease occurred at the northernmost tip of the terminus and the upper part of the glacier outlet where the ice starts flowing out of the caldera (Fig. 11C). Elevation differences between 2021 and 2024 mostly reveal an overall but slight thinning of Gígjökull, with the exception of the lowermost part where ice thickening of between 10 and 50 m occurred (Fig. 11D).

Cross sections provide a more detailed overview of elevations in individual years (Fig. 12). Starting with the lava emplacement in the caldera (A-A‘), data show that elevation gain only happened toward the edges of the lava pile between 2010 and 2014, but the center remained at the same elevation. Elevation increase is visible from 2014 to 2024 (ca. 60 m in the center). However, the elevation is still 20–30 m below the pre-eruption level from 2008. Cross sections further down (to the north of) the outlet glacier (B-B’,C-C’, D-D’) reveal a very similar pattern. Cavities quickly started refilling and significantly increased in elevation by 2014, in some areas up to 100 m. Elevations in 2021 and 2024 were nearly identical and very similar to those from 2014, although minor disparity is visible. In all cases, the level from 2008 prior to the eruption has not been reached by 2024. Cross section E-E’ displays the end of the subglacial lava flow. There was little elevation change prior to 2014. However, elevations in 2021 and 2024 nearly reached the 2008 level. The last section (F-F’) represents the situation of the glacier terminus. Data reflect the alternating behavior of the terminus with elevation increase and loss as illustrated in Fig. 11.

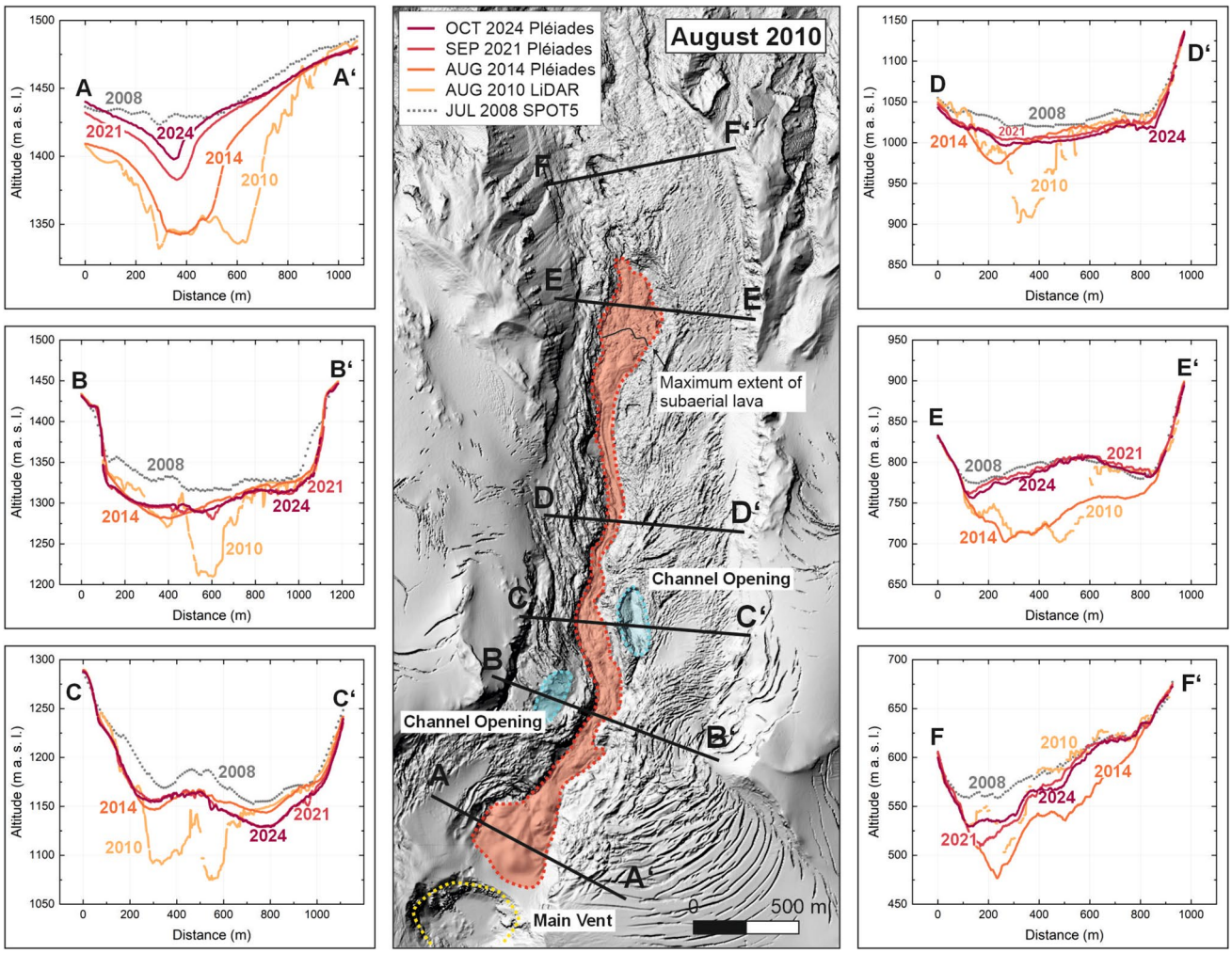

Fig. 12 Cross sections of the outlet glacier Gígjökull and the northern part of the summit caldera

Recent observations of the ice cap (summer and autumn 2024)

On-site visits of the summit caldera and overflights in summer and autumn 2024 resulted in two major observations: (i) A small depression was still visible in the area of subglacial lava emplacement, but all other visible signs of the eruption have vanished in the caldera; (ii) a new depression in the northern part of the caldera has formed (Fig. 13). Aerial photographs from October 2024 show a depression closely located to the breach in the caldera rim where Gígjökull emerges (Fig. 13C). As no signs were visible during a previous overflight in July nor during an on-site visit in August (Fig. 13A, B), the depression must have formed between August and October 2024. A depression was observed at the same location in 2012 (Fig. 2) but vanished shortly afterwards. The elevation change in this area and the formation of a circular shape is also clearly visible in Fig. 6D, indicating a loss of ca. 10 m between 2021 and 2024. During the on-site visit in August, substantial tephra accumulations were visible at the western edges of the glacier, often piled up into small heaps, or otherwise mixed with snow, letting large parts of the surface area appear black (Appendix C).

Discussion

Recovery of individual areas after the eruption

During the eruption, different areas of the ice cap were subjected to volcano-ice interactions of varying duration and severity. These variations strongly correlate with the recovery time of individual areas and their development after 2010. While visible eruption impacts on the southern flank vanished completely (nothing was visible in 2014) and the glacier only needed a short time to reach the pre-eruption state, minor signs in the form of a small depression were still visible in the summit caldera during on-site investigations

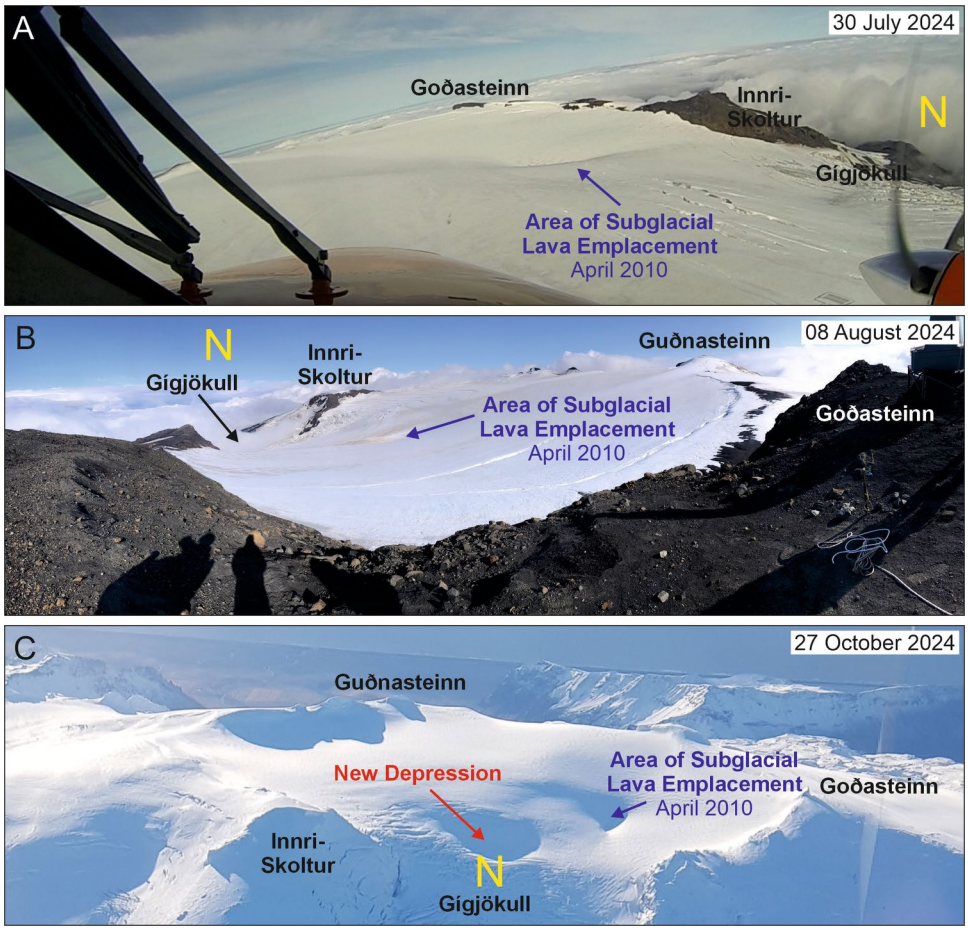

Fig. 13 State of the summit caldera in July, August, and October 2024 and evolution of a new depression close to Gígjökull. **A** Aerial photograph taken on 30 July 2024. Viewing direction is to the west. **B** View into the summit caldera from Goðasteinn. Photomosaic was taken on 8 August 2024. **C** Aerial photograph taken on 27 October 2024 by Ethienne Berthier. Viewing direction is to the south. N indicates north in all photographs

in summer/autumn 2024 and on Pléiades satellite imagery from October 2024. Similar to the eruption fissure on the southern flank, Gígjökull also revealed a fast recovery and quickly returned to alternating phases of advance and retreat as observed prior to the eruption (Sigurdsson 1998; Strachan 2001).

There are two main factors influencing the recovery of individual areas: (i) the amount of residual heat (e.g., lava, pyroclasts, and lakes) and its decline over time and (ii) the location of disruption on the ice cap. It is also relevant to consider the amount of ice that melted during the eruption, the depth of individual structures within the ice cap, and the duration of activity of individual sites. The eruption fissure on the southern flank was only active for 1 day and created a cavity up to ~ 60 m deep (Fig. 9A). Compared to the other areas, the impact of the eruption was rather small and much of the meltwater had drained out as a supraglacial flood in the beginning of activity due to the thinner ice cover (50–100 m) and the steep terrain (Magnusson et al., 2012). The fast recovery suggests that the heat source in this location was exhausted very quickly, probably reflecting a shallow, lateral propagation of the magma erupting here on the first day of the eruption. Both ice melting and heat output were significantly higher in the caldera and steaming was at least visible up to ~ 3 years after the eruption at the main vent (Fig. 5F) with elevation change/loss of up to 160 m; 80-m loss was observed in the area where lava flow emplacement (initially subglacially) started (Figs. 6A, 7B, and 12A-A'). Other factors such as a changing albedo due to the tephra coverage might have influenced the ice cap as well. However, we assume that this was mostly relevant immediately after the eruption and in the summer of 2010. After that time, most areas were covered by snow again (Figs. 5 and 8).

Differences between the recovery time of the main and minor vent are clearly a result of the duration of activity and degree of interference. Disparities between the main vent and the area of lava accumulation, however, are primarily related to different heat capacities. Oddsson et al. (2016a) determined a lava heat capacity of $1.0*10^3$ J kg^{-1} K^{-1}. Experiments carried out by Stroberg et al. (2010) found heat capacities ranging between 8.2 and $8.7*10^2$ J kg^{-1} K^{-1} for volcanic clasts.

It was estimated that the subglacial lava already lost 45% of its thermal energy for ice melting and another 5% was lost to the atmosphere and heating of water during the eruption and that the majority of the calculated residual

heat of $4.1 \pm 1.7*10^{16}$ J was stored in the thickest part of the lava which was emplaced in the caldera (Oddsson et al. 2016b). If this residual heat had all been used for basal melting since the end of the eruption, the melted ice would be ~ 1.4×10^8 m^3, which is almost double the volume gain of the Gígjökull ice catchment between 2010 and 2024, and corresponds to ~ 1.4 m lowering of this area overall over this time span. This is unlikely the case since it would imply that the surface mass balance of Gígjökull was extremely high, not only ~ 1 m water equivalent/year like the geodetic results indicate, without basal melting, but more like 2–3 m water equivalent/year to compensate for the basal melting. It is more likely that the surface mass balance of Gígjökull was somewhere in the range of 1–2 m water equivalent/year during this period. Basal melt substantially lower than ~ 1.4×10^8 m^3 in 2010–2024 may be caused by several reasons and likely a combination of more than one including the following: (i) The residual heat of the lava at the end of the eruption being overestimated; (ii) significant further amount of heat has been lost into the atmosphere and heating of water percolating through the lava without getting into further contact with the glacier and therefore not causing ice melt; (iii) a significant proportion of the residual heat in 2010 is still being stored in the lava.

The pyroclastic deposits confining the two vents lost most of their remaining heat during or immediately after the eruption (after becoming inactive). A significant amount was likely lost to the atmosphere through steaming; another part was probably used for melting snow and heating of water in the main vent (lake formation, Fig. 5C). It is likely that the minor vent lost most of its energy after becoming inactive and even before the eruption ended, as no significant steaming is visible on post-eruption images. The order of recovery from fast to slow is as follows: (i) southern flank eruption fissure, (ii) minor vent, (iii) main vent, and (iv) subglacial lava (caldera).

Similar to the eruption fissure on the southern flank and the caldera, Gígjökull also revealed a fast recovery with a lot of elevation increase by 2014 and an advancing glacier terminus since at least 2019, after a period of retreat observed since 2014. At Gígjökull, heat loss at the lava happened much faster than in the caldera. First, the lava was much thinner, and second, the influence of meltwater was much greater (Oddsson et al. 2016b). This in turn means the lava at Gígjökull was not able to store a lot of heat after the eruption ended and cooled comparatively fast, thus not preventing new snow/ice from accumulating on top of it.

Development of eruption sites versus overall glacier response

Glaciers globally (IPCC 2021) and in Iceland (Hannesdóttir et al. 2020; Gudmundsson et al. 2025) are retreating. The Eyjafjallajökull ice cap is following the same trend as shown by a persistent area decrease between 2010 and 2024 and continuous volume loss (Table 1). However, the areas impacted by the eruption were able to significantly recover and showed a strongly positive mass balance in the years following the eruption. We hypothesize that these differences between the caldera/Gígjökull and the rest of the ice cap can be explained by the morphology changes of the caldera after the eruption. The caldera, which feeds Gígjökull (Gígjökull ice catchment), had significantly changed after 2010. Major depressions had formed where the eruption vents were and lava was emplaced. These depressions likely acted as traps for drifting snow in winter, resulting in a local thickening rate far exceeding the average winter accumulation. Without these depressions and also considering the high wind speeds at the summit, it is likely that the snow would have been deposited on other parts of the ice cap. Another factor that has to be considered is the altitude. The eruption took place in the uppermost part of the ice cap, which is (so far) less impacted by rising temperatures and serves as an accumulation area for Gígjökull. However, the altitude likely played a secondary role. There are several outlet glaciers in Iceland with similar conditions and even higher feeding areas. None of them showed a comparable volume increase (positive mass balance). Öræfajökull, for example, has very similar conditions as Gígjökull, but with a caldera that is ~ 300 m higher than the one of Eyjafjallajökull. Between 2010 and 2017, it experienced a positive mass balance. However, with ~ 0.2 m water equivalent/year (Belart et al. 2020), it was far less than what we observed at Gígjökull. Other outlet glaciers in Iceland predominantly experienced negative mass balances between 2010 and 2024. This supports our assumption that the altitude cannot be the main factor responsible for the fast recovery of the eruption sites.

Although a positive mass balance was observed at the Gígjökull ice catchment after the eruption and visible eruption impacts started to disappear, the ice cap did not reach the pre-eruption state by autumn 2024. Studies by Magnússon et al. (2012) and Oddsson et al. (2016b) revealed a total volume loss of ~ 200 m^3 related to the eruption. A comparison to the total volume gain that was achieved between August 2010 and October 2024 (~ 100 m^3) shows that this surplus is still only 50% of the overall volume that was lost during the eruption. Since we hypothesize that the depressions played a major role for snow accumulation immediately after the eruption and strongly impacted the fast recovery, we can assume that this process will be slowing down in the coming years as the depressions become shallower and less snow will be trapped. This will likely reduce the contrast in mass balance between the Gígjökull ice catchment and the rest of the ice cap.

While the eruption severely impacted specific areas of the ice cap, resulting in ice melt and substantial morphology

changes, large parts of the volcanic flanks were impacted by a tephra layer. This probably affected the ice cap in the first 1–2 years after the eruption, either due to a changed albedo or insulating effects, but likely less in the long-term since the tephra got covered by snow afterwards. Although here we cannot quantify the impacts the eruption had on the volcanic flanks in the longer term, we think that negative effects could have been caused by less snow reaching these areas due to the high accumulation in the caldera. Tephra that was deposited on the flanks in 2010 was still visible at the glacier margins during field visits in August 2024 (Appendix C) as a result of ice movement and melt. These accumulations can influence the pathways of supraglacial meltwater channels and probably have both insulating effects in areas with sufficient material and enhanced melting effects where the ice is covered by a very thin and patchy layer.

Future development of the ice cap

A national glacier inventory for Iceland by Hannesdóttir et al. (2020) provides clear evidence that most of the Icelandic glaciers started retreating in ~ 1995 due to rising temperatures—after a period of stagnation or even readvancing after ~ 1960. The Eyjafjallajökull ice cap follows these trends and is currently retreating, although areas impacted by the eruption were able to significantly recover since 2010. Assuming that temperatures will further increase in the future it is likely that the areas already impacted by climate change will continue to decrease. The edges of the ice cap will continue to thin and the areal extent will diminish. The summit caldera will likely remain in its current state with only minor changes over the next few decades, unless temperature increase will be strong enough to affect higher altitudes or substantial changes in precipitation will arise. However, since the depressions likely played a major role for the strong positive mass balance, we can assume that snow accumulation will decrease along with the disappearance of the depressions, which will therefore affect the future of Gígjökull. Although the ice cap notably recovered from the eruption impacts and the Gígjökull ice catchment might experience a continued positive mass balance in the next few years, it is unlikely that the total volume that was lost during the eruption will be replenished or the overall ice cap will continue to advance again under the current conditions. In the event of an eruption as observed in 2010, the ice cap might be able to recover, although this strongly depends on the area that will be impacted, the magnitude of the eruption, and the morphology changes that are left behind.

Volcano-glacier interactions and glacier recovery on a global scale

Although global warming causes worldwide glacier retreat, we find that volcanic eruptions do not necessarily accelerate this process in the long term (first few decades after the eruption). Even though they usually impact the ice cover during an eruption and can lead to substantial melting, the long-term consequences strongly depend on the type of eruption, the location of eruption sites on the volcanic edifice/ice cover, and several external factors (e.g., wind, precipitation, and shade). Notable morphology changes in the aftermath of an eruption can even cause a new glacier to form and survive subsequent activity periods as observed in the horseshoe-shaped crater of Mount St. Helens (Schilling et al. 2004; Walder et al. 2008). Other studies found that even direct interactions between lava and snow/ice do not always cause immediate melting due to the effective thermal insulation between the incandescent lava and the underlying snow/ice. This was observed during the 2010 Fimmvörðuháls eruption, Iceland (Edwards et al. 2012), and again in 2018 at Mount Veniaminof, Alaska, USA (Waythomas et al. 2022). However, long-term impacts can arise as a consequence of immense volcano-ice interactions during an eruption affecting large parts of the ice cap. A famous example is the disastrous 1985 eruption of Nevado del Ruiz, Columbia, where the eruption significantly determined the future development of the ice cap and led to substantial degradation (Thouret et al. 2007). Ultimately, there are several factors determining whether an eruption causes long-term impacts on the glacier cover or not. Barr et al. (2018) present several examples of volcanic impacts on modern glaciers (since AD 1800) and concluded that shorter-term (days-to-months) impacts are typically destructive, while longer-term (years-to-decades) are more likely protective (e.g., limiting climatically driven ice loss).

Conclusions

The 2010 summit eruption of Eyjafjallajökull caused considerable melting in the caldera, forming ice cauldrons over 160-m deep. Some melting occurred on the upper part of the southern flank, but the event was short-lived with comparatively little impact. The propagation of an initially subglacial lava flow down Gígjökull severely impacted the outlet glacier, formed ice canyons, and melted substantial parts of it. Since glaciers in Iceland are retreating, it is surprising that the areas impacted by the eruptions were able to start recovering so quickly and experience a positive mass balance, unlike the rest of the ice cap. Although the altitude (summit eruption) contributed to the fast recovery, it likely played a secondary role. We rather propose the morphology changes in the caldera were the key factor for the extremely positive mass balance. Depressions formed during the eruption likely acted as traps for drifting snow in winter, resulting in a local thickening rate exceeding the average winter accumulation. Without these morphology

changes, snow would have been transported to other parts of the ice cap by wind. Since the eruption impact strongly varied between eruption sites, the recovery times showed differences as well. Apart from the impact of the eruption itself and the duration, the differences in residual heat also affected the recovery time. While the short-lived eruption fissure on the southern flank lost all its heat very quickly and snow accumulation started even while the eruption at the summit was ongoing, heat remained much longer at the vents and the thick body of lava, which started to accumulate subglacially. As a conclusion, we can say that the fast recovery of Eyjafjallajökull is surprising and not what you would expect from a glacier with remaining heat sources caused by an eruption, forms of geothermal activity as indicated by the sporadic appearance of the small cauldron in the northern part of the caldera, and a negative mass balance experienced by almost all other Icelandic outlet glaciers. However, despite the recovery, the Gígjökull ice catchment has not fully recovered and only regained ~ 50% of the volume that was lost during the eruption. If the eruption happened at other parts of the ice cap, a recovery as seen here would probably not have been possible. In the long term, the eruption clearly impacted the subglacial morphology of the caldera, Gígjökull, and the southern flank. Overall, the ice cap was impacted by less snow accumulation, as substantial parts were trapped in the caldera. Although we cannot quantify how the ice cap would have evolved without being impacted by the eruption, it is unlikely that a positive mass balance over the last years would have been reached while all other ice caps showed retreat.

Supplementary Information The online version contains supplementary material available at https://doi.org/10.1007/s00445-026-01995-5.

Acknowledgements We would like to thank the two anonymous reviewers for their useful comments and suggestions for improving the manuscript. Thanks to Hrafnhildur Hannesdóttir for providing glacier outlines.

Author contributions LS and EM conceptualized and wrote the draft. All authors contributed to the text, the writing and editing process, reviews, and provided feedback. JMCB pre-processed the SPOT5 and Pléiades data. EM conducted the volume calculations. LS prepared all figures.

Funding Open access funding provided by University of Iceland. This project was funded by the Icelandic Research Fund (Rannís) under grant number 2410268-051.

Data Availability The SPOT5 and Pléiades images have data access restrictions. The LiDAR data are available upon request to the authors (Jóhannesson et al., 2013). Original glacier outlines are available upon request to the authors (Belart et al., 2020; Hannesdóttir et al., 2020) or available at Jöklavefsjá (https://islenskirjoklar.is/#/page/map). Maps of elevation difference and modified glacier outlines are published at Zenodo (https://doi.org/10.5281/zenodo.20529384). All photographs were taken by the authors and are available upon request.

Declarations

Competing interests The authors declare no competing interests.

References

Adalgeirsdóttir G, Magnússon E, Pálsson F, Thorsteinsson T, Belart JMC, Jóhannesson T, Hannesdóttir H, Sigurðsson O, Gunnarsson A, Einarsson B, Berthier E, Schmidt LS, Haraldsson HH, Björnsson H (2020) Glacier changes in Iceland from ~1890 to 2019. Front Earth Sci 8:523646. https://doi.org/10.3389/feart.2020.523646

Barr ID, Lynch CM, Mullan D, de Siena L, Spagnolo M (2018) Volcanic impacts on modern glaciers: a global synthesis. Earth-Sci Rev 182:186–203. https://doi.org/10.1016/j.earscirev.2018.04.008

Belart JMC, Magnússon E, Berthier E, Pálsson F, Adalgeirsdóttir G, Jóhannesson T (2019) The geodetic mass balance of Eyjafjallajökull ice cap for 1945–2014: processing guidelines and relation to climate. J Glaciol 65(251):395–409. https://doi.org/10.1017/jog.2019.16

Belart JMC, Magnússon E, Berthier E, Gunnlaugsson ÁÞ, Pálsson F, Adalgeirsdóttir G, Jóhannesson T, Thorsteinsson T, Björnsson H (2020) Mass balance of 14 Icelandic glaciers, 1945–2017: spatial variations and links with climate. Front Earth Sci. https://doi.org/10.3389/feart.2020.00163

Berthier E, Vincent C, Magnússon E, Gunnlaugsson ÁÞ, Pitte P, le Meur E, Masiokas M, Ruiz L, Pálsson F, Belart JMC, Wagnon P (2014) Glacier topography and elevation changes derived from Pléiades sub-meter stereo images. Cryosphere 8(6):2275–2291. https://doi.org/10.5194/tc-8-2275-2014

Björnsson H, Pálsson F (2008) Icelandic glaciers. Jökull 58(1):365–386. https://doi.org/10.33799/jokull2008.58.365

Björnsson H (2017) Iceland. In: The glaciers of Iceland. Atlantis Advances in Quaternary Science, 2. Atlantis Press, Paris. https://doi.org/10.2991/978-94-6239-207-6_3

Crochet P (2007) A study of regional precipitation trends in Iceland using a high-quality gauge network and ERA-40. J Clim 20(18):4659–4677. https://doi.org/10.1175/JCLI4255.1

Dürig T, Gudmundsson MT, Ágústsdóttir T, Högnadóttir T, Schmidt LS (2022) The effect of wind and plume height reconstruction methods on the accuracy of simple plume models — a second look at the 2010 Eyjafjallajökull eruption. Bull Volcanol 84(3):33. https://doi.org/10.1007/s00445-022-01541-z

Edwards B, Magnússon E, Thordarson T, Gudmundsson MT, Höskuldsson A, Oddsson B, Haklar J (2012) Interactions between lava and snow/ice during the 2010 Fimmvörðuháls eruption, south-central Iceland. J Geophys Res Solid Earth. https://doi.org/10.1029/2011JB008985

Einarsson P, Sæmundsson K (1987) Earthquake epicenters 1982–1985 and volcanic systems in Iceland (map). In: Sigfússon Th (ed) Í hlutarins eðli: Festschrift for Þorbjörn Sigurgeirsson. Reykjavík, Menningarsjóður

Guðmundsson S, Magnússon E, Belart JMC, Hannesdóttir H, Aðalgeirsdóttir G (2025) The fate of two Icelandic glaciers in warming climate: Hofsjökull eystri and Okjökull. Annals of Glaciology 66:e36. https://doi.org/10.1017/aog.2025.10026

Gudmundsson MT, Larsen G, Höskuldsson Á, Gylfason ÁG (2008) Volcanic hazards in Iceland. Jökull 58(1):251–268. https://doi.org/10.33799/jokull2008.58.251

Gudmundsson AT (1996) Volcanoes in Iceland: 10,000 years of volcanic history. Vaka-Helgafell, Reykjavik. pp 136. https://www.abebooks.com/9789979203483/Volcanoes-Iceland-000-Years-Volcanic-997920348X/plp

Gudmundsson MT, Pedersen R, Vogfjörd K, Thorbjarnardóttir B, Jakobsdóttir S, Roberts MJ (2010) Eruptions of Eyjafjallajökull Volcano, Iceland. Eos, Transactions American Geophysical Union 91(21):190–191. https://doi.org/10.1029/2010EO210002

Hannesdóttir H, Sigurdsson O, Þrastarson RH, Gudmundsson S, Belart JMC, Pálsson F, Magnússon E, Víkingsson S, Jóhannesson T (2020) A national glacier inventory and variations in glacier extent in Iceland from the Little Ice Age maximum to 2019. Jökull 70(1):1–34. https://doi.org/10.33799/jokull2020.70.001

Hjaltadóttir S, Vogfjörð KS, Slunga R (2009) Seismic signs of magma pathways through the crust in the Eyjafjallajökull volcano, south Iceland. Rep. VI 2009–13, Icelandic Meteorol. Off., Reykjavík, pp 33. https://en.vedur.is/earthquakes-and-volcanism/reports-and-publications/chrome-extension://efaidnbmnnnibpcajpcglclefindmkaj/https://www.vedur.is/media/vedurstofan/utgafa/skyrslur/2009/VI_2009_013.pdf

Intergovernmental Panel on Climate Change (IPCC) (2023) Climate change 2021 – the physical science basis. Contribution of Working Group I to the Sixth Assessment Report of the Intergovernmental Panel on Climate Change. Cambridge University Press. https://doi.org/10.1017/9781009157896

Jakobsson S, Jónasson K, Sigurðsson IA (2008) The three igneous rock series of Iceland. Jökull 58(1):117–138. https://doi.org/10.33799/jokull2008.58.117

Jarosch A, Gudmundsson MT, Högnadóttir T, Axelsson G (2008) Progressive cooling of the hyaloclastite ridge at Gjálp, Iceland, 1996–2005. J Volcanol Geotherm Res 170(3–4):218–229. https://doi.org/10.1016/j.jvolgeores.2007.10.012

Jóhannesson T, Björnsson H, Magnússon E, Guðmundsson S, Pálsson F, Sigurðsson O, Thorsteinsson T, Berthier E (2013) Ice-volume changes, bias estimation of mass-balance measurements and changes in subglacial lakes derived by lidar mapping of the surface of Icelandic glaciers. Annals of Glaciology 54(63):63–74. https://doi.org/10.3189/2013AoG63A422

Loughlin SC (2002) Facies analysis of proximal subglacial and proglacial volcaniclastic successions at the Eyjafjallajökull central volcano, southern Iceland. In: Smellie JL, Chapman MG (eds) Volcano Ice Interactions on Earth and Mars: Geol Soc Spec Publ 202:149–178

Larsen G (2000) Holocene eruptions within the Katla volcanic system, south Iceland: characteristics and environmental impact. Jokull 49(1):1–28. https://doi.org/10.33799/jokull2000.49.001

Magnússon E, Gudmundsson MT, Roberts MJ, Sigurðsson G, Höskuldsson F, Oddsson B (2012) Ice-volcano interactions during the 2010 Eyjafjallajökull eruption, as revealed by airborne imaging radar. J Geophys Res Solid Earth. https://doi.org/10.1029/2012JB009250

Magnússon E, Muñoz-Cobo Belart J, Pálsson F, Ágústsson H, Crochet P (2016) Geodetic mass balance record with rigorous uncertainty estimates deduced from aerial photographs and lidar data – case study from Drangajökull ice cap, NW Iceland. Cryosphere 10(1):159–177. https://doi.org/10.5194/tc-10-159-2016

Oddsson B, Gudmundsson MT, Sonder I, Zimanowski B, Schmid A (2016a) Experimental studies of heat transfer at the dynamic magma ice/water interface: application to subglacially emplaced lava. J Geophys Res Solid Earth 121(5):3261–3277. https://doi.org/10.1002/2016JB012865

Oddsson B, Gudmundsson MT, Edwards BR, Thordarson T, Magnússon E, Sigurðsson G (2016b) Subglacial lava propagation, ice melting and heat transfer during emplacement of an intermediate lava flow in the 2010 Eyjafjallajökull eruption. Bull Volcanol 78(7):48. https://doi.org/10.1007/s00445-016-1041-4

Oskarsson BV (2009) The Skerin ridge on Eyjafjallajökull, south Iceland: morphology and magma-ice interaction in an ice-confined silicic fissure eruption. MS thesis, University of Iceland, Reykjavík, Iceland. https://skemman.is/handle/1946/4375?locale=en

Pedersen R, Sigmundsson F (2004) InSAR based sill model links spatially offset areas of deformation and seismicity for the 1994 unrest episode at Eyjafjallajökull volcano, Iceland. Geophys Res Lett 31(14):2004GL020368. https://doi.org/10.1029/2004GL020368

Reynolds HI, Gudmundsson MT, Högnadóttir T, Pálsson F (2018) Thermal power of Grímsvötn, Iceland, from 1998 to 2016: quantifying the effects of volcanic activity and geothermal anomalies. J Volcanol Geotherm Res 358:184–193. https://doi.org/10.1016/j.jvolgeores.2018.04.019

Ripepe M, Bonadonna C, Folch A, Delle Donne D, Lacanna G, Marchetti E, Höskuldsson A (2013) Ash-plume dynamics and eruption source parameters by infrasound and thermal imagery: the 2010 Eyjafjallajökull eruption. Earth Planet Sci Lett 366:112–121. https://doi.org/10.1016/j.epsl.2013.02.005

Schilling SP, Carrara PE, Thompson RA, Iwatsubo EY (2004) Posteruption glacier development within the crater of Mount St. Helens, Washington, USA. Quat Res 61:325–329. https://doi.org/10.1016/j.yqres.2003.11.002

Shevchenko A, Walter TR, Gudmundsson MT, Belart JMC, Marzban P, Zorn EU, Sæmundsson Þ, Helgason JK, Turowski JM, Vassileva MS, Motagh M, Müller D (2024) Morphological changes of the south-eastern wall of Askja caldera, Iceland over the past 80 years. Commun Earth Environ 5(1):441. https://doi.org/10.1038/s43247-024-01616-z

Sigmundsson F, Hreinsdóttir S, Hooper A, Árnadóttir T, Pedersen R, Roberts MJ, Óskarsson N, Auriac A, Decriem J, Einarsson P, Geirsson H, Hensch M, Ófeigsson BG, Sturkell E, Sveinbjörnsson H, Feigl KL (2010a) Intrusion triggering of the 2010 Eyjafjallajökull explosive eruption. Nature 468(7322):426–430. https://doi.org/10.1038/nature09558

Sigmundsson F, Pinel V, Lund B, Albino F, Pagli C, Geirsson H, Sturkell E (2010b) Climate effects on volcanism: influence on magmatic systems of loading and unloading from ice mass variations, with examples from Iceland. Philos Trans R Soc A Math Phys Eng Sci 368(1919):2519–2534. https://doi.org/10.1098/rsta.2010b.0042

Sigurdsson O (1998) Glacier variations in Iceland 1930-1995 - from the database of the Iceland Glaciological Society. Jokull 45:3–26

Spinetti C, Barsotti S, Neri A, Buongiorno MF, Doumaz F, Nannipieri L (2013) Investigation of the complex dynamics and structure of the 2010 Eyjafjallajökull volcanic ash cloud using multispectral

images and numerical simulations. J Geophys Res Atmos 118(10):4729–4747. https://doi.org/10.1002/jgrd.50328
Stroberg TW, Manga M, Dufek J (2010) Heat transfer coefficients of natural volcanic clasts. J Volcanol Geotherm Res 194(4):214–219. https://doi.org/10.1016/j.jvolgeores.2010.05.007
Strachan SM (2001) A geophysical investigation of the Eyjafjallajökull glaciovolcanic system, South Iceland, using radio echo sounding, PhD thesis, Department of Geography, University of Edinburgh, Edinburgh, UK. https://era.ed.ac.uk/bitstream/handle/1842/23212/StrachanSM_2001redux.pdf?sequence=1&isAllowed=y
Sturkell E, Einarsson P, Sigmundsson F, Hooper A, Ófeigsson BG, Geirsson H, Ólafsson H (2010) 2 Katla and Eyjafjallajökull Volcanoes. pp 5–21. https://doi.org/10.1016/S1571-0866(09)01302-5
Thouret JC, Ramírez C. J, Gibert-Malengreau B, Vargas CA, Naranjo JL, Vandemeulebrouck J, Valla F, Funk M (2007) Volcano–glacier interactions on composite cones and lahar generation: Nevado del Ruiz, Colombia, case study. Ann Glaciol 45:115–127. https://doi.org/10.3189/172756407782282589
Thoroddsen T (1925) Die Geschichte der isländischen Vulkane. Kongelige Danske Videnskabernes Selskab Skrifter, Naturvidenskabelig og Matematisk Afdeling, 8, Raekke, IX, Copenhagen, pp 458
Waythomas CF, Dietterich HR, Tepp GM, Lopez TM, Loewen MW (2022) The 2018 eruption of Mount Veniaminof. Alaska. https://doi.org/10.3133/sir20225075
Woodhouse MJ, Hogg AJ, Phillips JC, Sparks RSJ (2013) Interaction between volcanic plumes and wind during the 2010 Eyjafjallajökull eruption, Iceland. J Geophys Res Solid Earth 118(1):92–109. https://doi.org/10.1029/2012JB009592
Walder SJ, Schilling SP, Vallance JW, LaHusen RG (2008) Effects of lava-dome growth on the crater glacier of Mount St. Helens, Washington. In: Sherrod, D. R., Scott, W. E., Stauffer, P. H. (eds) A volcano rekindled: the renewed eruption of Mount St. Helens, 2004–2006: U.S. Geological Survey Professional Paper 1750, pp 257–273